

11-02
380 346

TECHNICAL MEMORANDUM

X-119

AERODYNAMIC LOADING CHARACTERISTICS INCLUDING EFFECTS OF
AEROELASTICITY OF A THIN-TRAPEZOIDAL-WING-BODY
COMBINATION AT A MACH NUMBER OF 1.43

By Thomas C. Kelly

Langley Research Center
Langley Field, Va.

Declassified September 1, 1961

NATIONAL AERONAUTICS AND SPACE ADMINISTRATION
WASHINGTON

September 1959

NATIONAL AERONAUTICS AND SPACE ADMINISTRATION

TECHNICAL MEMORANDUM X-119

AERODYNAMIC LOADING CHARACTERISTICS INCLUDING EFFECTS OF
AEROELASTICITY OF A THIN-TRAPEZOIDAL-WING—BODY
COMBINATION AT A MACH NUMBER OF 1.43

By Thomas C. Kelly

SUMMARY

Results have been obtained in the Langley 8-foot transonic pressure tunnel at a Mach number of 1.43 and at angles of attack from 0° to about 24° which indicate the static-aerodynamic-loads characteristics for a 2-percent-thick trapezoidal wing in combination with a body. Included are the effects of changing Reynolds number and of fixing boundary-layer transition.

The results show that aerodynamic loading characteristics at a Mach number of 1.43 are similar to those reported in NACA RM L56J12a for the same configuration at a Mach number of 1.115. Reducing the Reynolds number resulted in reductions in the deflection of the wing and caused a slight increase in the relative loading over the outboard wing sections since the deflections were in a direction to unload the tip sections. Little or no effects were seen to result from fixing boundary-layer transition at a tunnel stagnation pressure of 1,950 pounds per square foot.

INTRODUCTION

A general research program in the Langley 8-foot transonic tunnels was established to determine the aerodynamic characteristics of wing-body combinations designed to have high lift-drag ratios at transonic and supersonic speeds. As one phase of this program, the aerodynamic loading characteristics at Mach numbers from 0.80 to 1.115 and the aerodynamic force characteristics at Mach numbers from 0.80 to 1.43 were obtained for a thin trapezoidal wing in combination with various bodies. These results are available in references 1 and 2, respectively.

The aerodynamic loading characteristics at a Mach number of 1.43 are given herein for some of the configurations reported in reference 1. Tests extended over an angle-of-attack range from 0° to about 24° at Reynolds numbers of 2.48×10^6 and 1.27×10^6 based on the wing mean aerodynamic chord.

SYMBOLS AND COEFFICIENTS

b	wing span
c	airfoil section chord, measured parallel to plane of symmetry
c_{av}	average wing chord, S/b
\bar{c}	wing mean aerodynamic chord
D	diameter
M	free-stream Mach number
l	body length
p	local static pressure
p_∞	free-stream static pressure
p_t'	free-stream total pressure
q_∞	free-stream dynamic pressure
r	radius
r_{av}	average body radius between wing-body leading-edge and trailing-edge junctures
S	wing area
t	thickness
x	distance from leading edge of wing or nose of body (positive rearward)
y	distance measured laterally from plane of symmetry

α	angle of attack of body center line
θ	meridian angle of body orifice station (At Row A, 0° . See fig. 1 and table II.)
C_p	pressure coefficient, $\frac{p - p_\infty}{q_\infty}$
$C_{p, \text{sonic}}$	pressure coefficient corresponding to local Mach number of 1
c_n	wing section normal-force coefficient, $\int_0^1 (C_{p,L} - C_{p,U}) d\left(\frac{x}{c}\right)$
$c_{m, c/4}$	wing section pitching-moment coefficient about $0.25c$, $\int_0^1 (C_{p,L} - C_{p,U}) \left(0.25 - \frac{x}{c}\right) d\left(\frac{x}{c}\right)$
$c_{m, \bar{c}/4}$	wing section pitching-moment coefficient about $0.25\bar{c}$, $c_{m, c/4} + c_n \left(\frac{x_{\bar{c}/4}}{c} - \frac{x_{c/4}}{c}\right)$
$C_{m, fw}$	body pitching-moment coefficient about $0.25\bar{c}$, based on wing area and \bar{c} , $\frac{2\pi l^2 D_{\max}}{S\bar{c}} \int_0^{1/4} \int_0^1 \cos \theta \frac{r}{r_{\max}} (C_{p,L} - C_{p,U}) \frac{x_{c/4} - x}{l} d\left(\frac{x}{l}\right) d\left(\frac{\theta}{2\pi}\right)$
$C_{N, w}$	wing normal-force coefficient, $\int_{\frac{r_{av}}{b/2}}^1 c_n \frac{c}{c_{av}} d\left(\frac{y}{b/2}\right)$
$C_{m, w}$	wing pitching-moment coefficient about $0.25\bar{c}$, $\int_{\frac{r_{av}}{b/2}}^1 c_{m, \bar{c}/4} \frac{c^2}{c_{av}\bar{c}} d\left(\frac{y}{b/2}\right)$
$C_{N, fw}$	body normal-force coefficient based on wing area, $\frac{2\pi l D_{\max}}{S} \int_0^{1/4} \int_0^1 \cos \theta \frac{r}{r_{\max}} (C_{p,L} - C_{p,U}) d\left(\frac{x}{l}\right) d\left(\frac{\theta}{2\pi}\right)$

C_N	total normal-force coefficient, $C_{N,w} + C_{N,fw}$
$C_m, \bar{c}/4$	total pitching-moment coefficient about $0.25\bar{c}$, $C_{m,w} + C_{m,fw}$
$C_{b,w}$	wing bending-moment coefficient, referred to body center line, $\int_{\frac{r_{av}}{b/2}}^1 \left(\frac{c_n}{c_{av}} \right) \left(\frac{y}{b/2} \right) d \left(\frac{y}{b/2} \right)$

Subscripts:

L	lower surface
U	upper surface
max	maximum

APPARATUS

Tunnel

The Langley 8-foot transonic pressure tunnel, in its standard configuration, is a single-return, rectangular, slotted-throat tunnel having controls that allow for the independent variation of Mach number, density, temperature, and humidity. For the present tests, the longitudinal slots were enclosed with fairings in order to provide a $M = 1.43$ test section. Details of the resulting nozzle shape and the test-section Mach number distribution are presented in reference 3.

Models

A three-view drawing of the wing-body configuration tested is shown in figure 1. The wing was trapezoidal in plan form and had 26.6° sweep-back of the quarter-chord line, an aspect ratio of 2.61, a taper ratio of 0.211, and 2-percent-thick symmetrical circular-arc airfoil sections parallel to the plane of symmetry, with the maximum thickness located at the midchord station. The wing was constructed of type 416 stainless steel.

The body of the configuration was designed by using Sears-Haack ordinates in order to obtain a body having minimum wave drag for a given length and volume. Design ordinates for the body are given in table I.

MEASUREMENTS AND ACCURACY

Measurements of the local static pressures over the configuration were made by use of about 137 orifices distributed over the upper and lower wing surfaces at three wing semispan locations and along five fuselage meridian rows. Orifice locations are given in table II. Pressure coefficients, determined from these pressure measurements, are estimated to be accurate within ± 0.005 and are presented in tables III to V.

Model angle of attack was measured by means of a strain-gage attitude transmitter located in the nose of the model and is estimated to be accurate within $\pm 0.1^\circ$. Calibrations of the tunnel with the test section empty indicate that local deviations from the average free-stream Mach number did not exceed 0.015 during these tests. (See ref. 3.) The average free-stream Mach number was held to within ± 0.003 of the nominal value shown in the figures.

Influence coefficients obtained from a static loading of the wing and presented in reference 1 may be used in conjunction with the experimental wing section data given herein in table VI to compute wing twist angles.

TESTS

The wing-body configuration and the body alone were tested at a Mach number of 1.43 through an angle-of-attack range from 0° to about 24° . Transition strips, when used, were fixed on the model at 10 percent of the wing chord and at 10 percent of the body length. The strips were approximately 0.1 inch wide and were composed of no. 120 carborundum grains set in a plastic adhesive. Tests of the wing-body configuration were conducted with transition both fixed and natural at a tunnel stagnation pressure of about 1,950 pounds per square foot. In addition, the transition-fixed configuration was tested at a stagnation pressure of about 1,000 pounds per square foot.

The body alone was tested with transition fixed at a stagnation pressure of 1,950 pounds per square foot. Test Reynolds numbers, based on the wing mean aerodynamic chord, for stagnation pressures of 1,950 pounds per square foot and 1,000 pounds per square foot were 2.48×10^6 and 1.27×10^6 , respectively.

RESULTS

The model aerodynamic loading characteristics are shown in the following figures:

Pressure coefficients for wing in presence of body. Effect of transition	2
Pressure coefficients for wing in presence of body. Effect of Reynolds number	3
Pressure coefficients for body in presence of wing. Effect of transition	4
Pressure coefficients for body in presence of wing. Effect of Reynolds number	5
Pressure coefficients for body alone	6
Spanwise load distributions	7
Normal-force and pitching-moment characteristics of wing-body configuration	8
Normal-force and pitching-moment characteristics of wing in the presence of the body	9
Variation of wing bending-moment coefficient with normal-force coefficient	10
Wing center-of-pressure locations	11
Part of total load carried by the wing	12

DISCUSSION

Pressure Distributions

Pressure distributions for the wing in the presence of the body (fig. 2) are similar to those noted at a Mach number of 1.115 in reference 1. The main effect of increasing Mach number from 1.115 to 1.43 consists of a general decrease in load carried by the wing sections at a given angle of attack, as would be expected. (Compare fig. 2 with figs. 4(f) and 4(g) of ref. 1.)

The removal of the transition particles (fig. 2) had little or no effect on the pressure distributions at a tunnel stagnation pressure of 1,950 pounds per square foot. It should be noted here that selection of the size of transition particles was based upon results presented in reference 4 and a tunnel stagnation pressure of 1,950 pounds per square foot. Observations of similar models while using the oil film technique described in reference 5 have indicated the presence of turbulent flow for conditions similar to those of the present tests. Although the pressure distributions presented in figure 3 are for the configuration with transition fixed, the possibility exists that at the lower tunnel pressure the transition strip was not capable of tripping the boundary layer. However, since increases in angle of attack are conducive to early transition, it is believed that the main differences in the pressure distributions over the outboard wing stations at the higher angles

of attack are caused by aeroelastic effects. Differences noted in the pressure distributions for the 0.20b/2 station near the leading edge (fig. 3) may be associated with differences in boundary-layer condition in this region.

Spanwise twist distribution for this same wing at a Mach number of 1.115 and an angle of attack of 20° presented in reference 1 indicates, as would be expected for a sweptback wing, that sizable angles of wing twist (about 1.25°) are developed which are in a direction to unload the outer wing sections. Since these elastic deformations of the wing are a direct function of the tunnel total pressure, it would be expected that the increased effective washout caused by the higher total pressures would result in a relative decrease in load carried by the outer wing sections. This effect of wing twist due to load, or aeroelasticity, is indicated by comparison of the results presented in figure 3 for the wing tested at both 1,950 pounds per square foot and 1,000 pounds per square foot. For a given angle of attack, the higher loads carried by the outboard section of the wing tested at the lower pressures indicate these sections are operating at local angles of attack somewhat higher than those for the wing tested at the higher pressure.

Pressure coefficients for the body in the presence of the wing indicate little or no effects resulting from fixing boundary-layer transition at a stagnation pressure of 1,950 pounds per square foot (fig. 4) or from varying Reynolds number (fig. 5).

Comparison of results for the body alone (fig. 6) with those for the body in the presence of the wing (fig. 4) indicates the usual increase in body loading resulting from the influence of the wing.

Spanwise Load Distributions

Spanwise load distributions (fig. 7) exhibit the same variation in shape as that noted at lower speeds in reference 1 and change from roughly elliptical in shape at the lower angles of attack to more nearly triangular at the higher angles.

The location of the wing-body juncture shown in figure 7 was obtained by taking a root-mean-square value of the body radius over the region of the fuselage intersected by the wing. The resulting value was $0.175b/2$.

Normal-Force and Pitching-Moment Characteristics

Normal-force and pitching-moment characteristics are presented for the complete configuration in figure 8 and for the wing in the presence

of the body in figure 9. Comparison of the results of the present tests with force results obtained for an identical configuration and reported in reference 2 indicates good agreement in the normal-force characteristics and only fair agreement in the pitching-moment characteristics.

A slight indication of the destabilizing pitching-moment curve break noted at the higher Mach numbers and normal-force coefficients of reference 1 appears at a Mach number of 1.43 for the wing-body combination. As was also noted in reference 1, no indication of this break is apparent in the curve for the wing in the presence of the body. As would be expected, the curves for the wing in the presence of the body (fig. 9) exhibit a decrease in the slope of the normal-force curve and an increase in stability level when compared with the curves for the wing-body combination (fig. 8).

Wing Bending Moments

For the exposed wing the variation with wing normal-force coefficient of the wing bending-moment coefficient referred to the body center line is presented in figure 10 and shows a near-linear increase in bending-moment coefficient with wing normal-force coefficient.

Center-of-Pressure Location

Lateral and chordwise center-of-pressure positions (fig. 11) exhibit variations similar to those shown for a Mach number of 1.115 in reference 1. Although not shown in figure 11, it would be expected that reductions in total pressure (or, conversely, increases in wing rigidity) would result in slight outboard and rearward movements of the wing center of pressure similar to those shown in reference 6 for wings which differed in rigidity. Tests of the present configuration conducted at the higher pressure would correspond to the flexible wing of reference 6, whereas those conducted at the lower pressure would correspond to the more rigid wing case because of the smaller resulting deformations.

Division of Load

The division of load between the wing and body is illustrated in figure 12 which shows that the wing carries about 78 percent of the total load at the lower normal-force coefficients. Increases in normal-force coefficient are accompanied by decreases in the percent of the load carried by the wing to a value of 74 percent at a normal-force coefficient of 1.07 (fig. 12).

CONCLUDING REMARKS

An investigation of a thin trapezoidal wing in combination with a body at a Mach number of 1.43 indicates that the aerodynamic loading characteristics at this Mach number are similar to those previously reported in NACA RM L56J12a for the same configuration at a Mach number of 1.115. Reducing the test Reynolds number by lowering the tunnel stagnation pressure resulted in reductions in deflections of the wing which caused a slight increase in the relative loading over the outboard wing sections since the deflections were in a direction to unload the tip sections. The effects of fixing boundary-layer transition were negligible for tests conducted at a tunnel stagnation pressure of 1,950 pounds per square foot.

Langley Research Center,
National Aeronautics and Space Administration,
Langley Field, Va., June 11, 1959.

REFERENCES

1. Kelly, Thomas C.: Transonic Wind-Tunnel Investigation of Aerodynamic-Loading Characteristics of a 2-Percent-Thick Trapezoidal Wing in Combination With Basic and Indented Bodies. NACA RM L56J12a, 1957.
2. Kelly, Thomas C.: Transonic Wind-Tunnel Investigation of the Low-Lift Aerodynamic Characteristics, Including Effects of Leading-Edge Droop and Thickness, of a Thin Trapezoidal Wing in Combination With Basic and Indented Bodies. NACA RM L57I04, 1957.
3. Matthews, Clarence W.: An Investigation of the Adaptation of a Transonic Slotted Tunnel to Supersonic Operation by Enclosing the Slots With Fairings. NACA RM L55H15, 1955.
4. Braslow, Albert L., and Knox, Eugene C.: Simplified Method for Determination of Critical Height of Distributed Roughness Particles for Boundary-Layer Transition at Mach Numbers From 0 to 5. NACA TN 4363, 1958.
5. Loving, Donald L., and Katzoff, S.: The Fluorescent-Oil Film Method and Other Techniques for Boundary-Layer Flow Visualization. NASA MEMO 3-17-59L, 1959.
6. Osborne, Robert S., and Mugler, J. P., Jr.: Effects of Wing Elasticity on the Aerodynamic Characteristics of a 45° Sweptback-Wing-Fuselage Combination Measured in the Langley 8-Foot Transonic Tunnel. NACA RM L52G23, 1952.

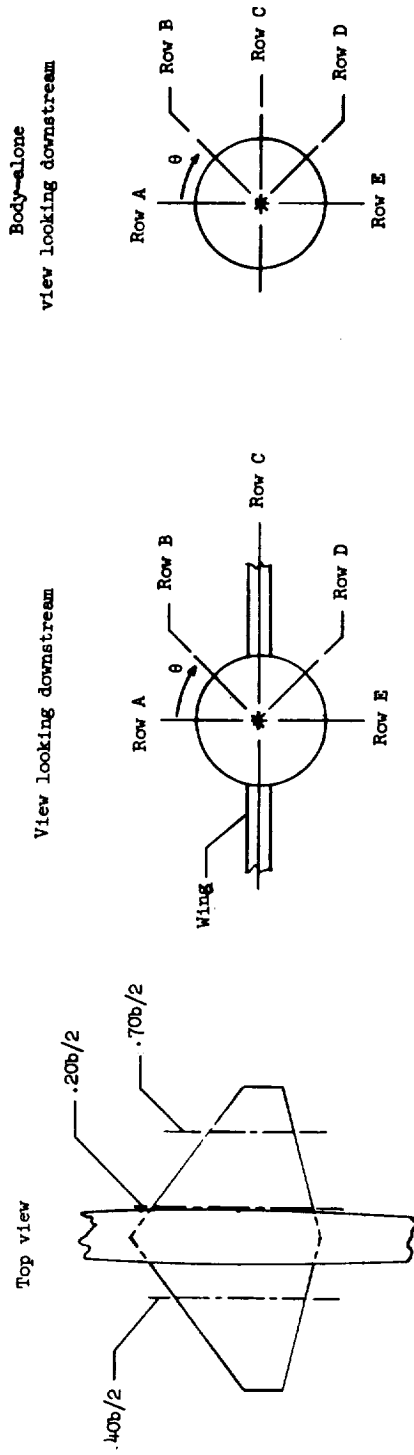
TABLE I

BODY ORDINATES

Body station, inches from nose	Body radius, in.
0	0
1.0	.282
2.0	.460
3.0	.612
4.0	.743
6.0	.969
8.0	1.150
10.0	1.290
12.0	1.404
13.426	1.475
14.0	1.493
16.0	1.552
18.0	1.590
20.0	1.606
22.0	1.594
24.0	1.560
26.0	1.501
28.0	1.414
30.0	1.300
32.0	1.158
34.0	.984
36.15	.750

Maximum body radius is 1.606 inches at body station 20.10 inches.

TABLE II.- MODEL ORIFICE LOCATIONS

Location of body orifices, x/l

Row A $\theta = 0^\circ$	Row B $\theta = 45^\circ$	Row C $\theta = 90^\circ$	Row D $\theta = 135^\circ$	Row E $\theta = 180^\circ$
0.055 .166 .277 .367 .402 .437 .472 .506 .541 .575 .610 .645 .676 .707 .748 .790 .831 .873 .954	0.166 .277 .367 .402 .437 .472 .506 .541 .575 .610 .645 .676 .707 .748 .790 .831 .873 .954	0.055 .166 .277 .367 .437 .472 .506 .541 .575 .610 .645 .676 .707 .748 .790 .831 .873 .954	0.166 .277 .367 .402 .437 .472 .506 .541 .575 .610 .645 .676 .707 .748 .790 .831 .873 .954	0.055 .166 .277 .367 .437 .472 .506 .541 .575 .610 .645 .676 .707 .748 .790 .831 .873 .954

Location of body orifices, x/l

Row A $\theta = 0^\circ$	Row B $\theta = 45^\circ$	Row C $\theta = 90^\circ$	Row D $\theta = 135^\circ$	Row E $\theta = 180^\circ$
0.055 .166 .277 .367 .387 .415 .443 .498 .553 .581 .636 .664 .692 .719 .775 .830 .871 .954	0.166 .277 .367 .387 .415 .443 .498 .553 .581 .609 .664 .692 .719 .775 .830 .871 .954	0.055 .166 .277 .367 .437 .472 .506 .541 .575 .610 .645 .676 .707 .748 .790 .831 .873 .954	0.166 .277 .367 .387 .415 .443 .498 .553 .581 .609 .664 .692 .719 .775 .830 .871 .954	0.055 .166 .277 .367 .437 .472 .506 .541 .575 .610 .645 .676 .707 .748 .790 .831 .873 .954

Location of wing pressure orifices, x/c

0.20b/2		0.40b/2		0.70b/2	
Upper surface	Lower surface	Upper surface	Lower surface	Upper surface	Lower surface
0.050 .075 .100 .150 .250 .350 .450 .550 .650 .750 .850 .900 .950	0.150 .250 .350 .450 .550 .650 .750 .850 .900 .950	0.075 .100 .150 .250 .350 .450 .550 .650 .750 .850 .900 .950	0.100 .150 .250 .350 .450 .550 .650 .750 .850 .900 .950	0.100 .150 .250 .350 .450 .550 .650 .750 .825 .900	0.150 .250 .350 .450 .550 .650 .750 .825 .900

TABLE III.- PRESSURE COEFFICIENTS FOR WING IN PRESENCE OF BODY

(a) Fixed transition; $p_t' = 1,950$ lb/sq ft

$\frac{x}{c}$	Upper surface			Lower surface			$\frac{x}{c}$	Upper surface			Lower surface		
	0.2b/2	0.4b/2	0.7b/2	0.2b/2	0.4b/2	0.7b/2		0.2b/2	0.4b/2	0.7b/2	0.2b/2	0.4b/2	0.7b/2
$\alpha = 0^\circ$							$\alpha = 8^\circ$						
0.050	0.003	0.072					0.050	-0.301	-0.327				
.075	.018				0.046		.075	-.260				0.394	
.100	.023	.017	0.082		.046		.100	-.234	-.336	-0.302		.372	
.150	.009		.040	-0.001	.034	0.085	.150	-.211		-0.301	0.268	.512	0.407
.250	-.016	.014	.031	-.007		.058	.250	-.209	-.313	-.294	.233		.339
.350	-.041	-.022	.008	.001	-.005	.019	.350	-.188	-.222	-.289	.181	.206	.280
.450	-.035	-.033	-.002	-.025	-.022	-.001	.450	-.174	-.205	-.290	.162	.189	.246
.550	-.053	-.053	-.042	-.041	-.032	-.022	.550	-.197	-.203	-.320	.174	.177	.223
.650	-.063	-.071	-.064	-.034	-.049	-.047	.650	-.213	-.206	-.333	.164	.172	.198
.750	-.052	-.070	-.079	-.059		-.058	.750	-.218	-.220	-.337	.133		.177
.825			-.080			-.066	.825			-.337			.154
.850	-.082	-.079		-.073	-.066		.850	-.230	-.227		.131	.134	
.900	-.094	-.080		-.082	-.071	-.062	.900	-.232	-.236		.120	.130	
.950	-.105	-.078					.950	-.235	-.235				.124
$\alpha = 2^\circ$							$\alpha = 12^\circ$						
0.050	-0.073	-0.053			0.135		0.050	-0.422	-0.456			0.614	
.075	-.053				.124		.075	-.369				.516	
.100	-.047	-.095	-0.013		.101	0.166	.100	-.340	-.446	-0.427		.454	0.536
.150	-.056		-.057	0.065		.134	.150	-.298		-.415	0.417		.469
.250	-.079	-.048	-.069	.044		.098	.250	-.270	-.430	-.403	.360	.342	.419
.350	-.083	-.085	-.091	.043	.050	.071	.350	-.251	-.378	-.395	.315	.311	.385
.450	-.078	-.087	-.092	.033	.038	.043	.450	-.234	-.297	-.389	.276	.302	.359
.550	-.097	-.093	-.116	.010	.017	.017	.550	-.241	-.275	-.410	.286	.293	.314
.650	-.093	-.103	-.122	.005	.001	.006	.650	-.259	-.273	-.412	.292	.293	.283
.750	-.106	-.114	-.134	-.008		.001	.750	-.265	-.277	-.419	.261		.270
.825		-.138					.825		-.416				
.850	-.131	-.122		-.018	-.024		.850	-.275	-.289		.243	.247	
.900	-.137	-.132		-.032	-.019	-.016	.900	-.283	-.292		.233	.242	.234
.950	-.148	-.130					.950	-.272	-.292				
$\alpha = 4^\circ$							$\alpha = 16^\circ$						
0.050	-0.141	-0.145			0.219		0.050	-0.528	-0.553			0.724	
.075	-.121				.215		.075	-.499				.649	
.100	-.115	-.179	-0.124		.174	0.249	.100	-.467	-.533	-0.524		.591	0.661
.150	-.119		-.130	0.126		.201	.150	-.358		-.509	0.569		.609
.250	-.118	-.122	-.145	.096		.148	.250	-.311	-.514	-.496	.500	.492	.560
.350	-.117	-.131	-.168	.078	.104	.128	.350	-.298	-.457	-.484	.467	.457	.516
.450	-.117	-.127	-.175	.072	.083	.108	.450	-.284	-.389	-.481	.425	.429	.475
.550	-.122	-.129	-.206	.067	.070	.076	.550	-.285	-.373	-.491	.416	.419	.423
.650	-.138	-.137	-.195	.048	.046	.064	.650	-.293	-.372	-.491	.416	.419	.391
.750	-.152	-.151	-.187	.029		.051	.750	-.305	-.374	-.495	.382		.368
.825		-.182					.825		-.490				
.850	-.165	-.164		.030	.026		.850	-.323	-.369		.336	.355	
.900	-.173	-.170		.014	.024	.025	.900	-.327	-.360		.330	.348	.335
.950	-.180	-.167					.950	-.332	-.349				
$\alpha = 6^\circ$							$\alpha = 20^\circ$						
0.050	-0.234	-0.248			0.298		0.050	-0.586	-0.602			0.854	
.075	-.202				.289		.075	-.562				.796	
.100	-.180	-.270	-0.225		.250	0.340	.100	-.442	-.593	-0.595		.746	0.782
.150	-.173		-.233	0.197		.268	.150	-.387	-.543	-.582	0.717		.725
.250	-.162	-.223	-.222	.168		.216	.250	-.361	-.535	-.569	.672	.633	.671
.350	-.167	-.175	-.236	.125	.156	.186	.350	-.333	-.484	-.556	.626	.595	.622
.450	-.145	-.170	-.245	.111	.137	.166	.450	-.291	-.468	-.552	.575	.562	.575
.550	-.167	-.172	-.275	.120	.125	.147	.550	-.305	-.484	-.560	.553	.527	.521
.650	-.185	-.175	-.282	.105	.108	.096	.650	-.324	-.504	-.556	.527	.476	.481
.750	-.192	-.195	-.287	.075			.750	-.347	-.477	-.557			.458
.825		-.274					.825		-.551				
.850	-.202	-.202		.081	.081		.850	-.361	-.432		.436	.453	
.900	-.209	-.207		.065	.076	.074	.900	-.371	-.420		.434	.436	.428
.950	-.216	-.204					.950	-.379	-.410				

TABLE III.- PRESSURE COEFFICIENTS FOR WING IN PRESENCE OF BODY - Continued

(b) Natural transition; $p_t' = 1,950$ lb/sq ft

$\frac{x}{c}$	Upper surface			Lower surface			$\frac{x}{c}$	Upper surface			Lower surface		
	0.2b/2	0.4b/2	0.7b/2	0.2b/2	0.4b/2	0.7b/2		0.2b/2	0.4b/2	0.7b/2	0.2b/2	0.4b/2	0.7b/2
$\alpha = 0^\circ$							$\alpha = 12^\circ$						
0.050	-0.001	0.075					0.050	-0.123	-0.460				
.075	.016				0.044		.075	-.370				0.602	
.100	.012	.003	0.061				.100	-.348	-.451	-0.438		.520	
.150	.008		.036	0.012	.037	0.091	.150	-.302		-.417	0.425	.460	0.526
.250	-.018	-.002	.020	-.007		.055	.250	-.273	-.433	-.405	.362		.460
.350	-.043	-.025	-.002	.003	.001	.019	.350	-.252	-.385	-.397	.312	.344	.415
.450	-.038	-.039	-.020	-.019	-.014	-.001	.450	-.233	-.305	-.395	.273	.310	.388
.550	-.053	-.054	-.049	-.039	-.027	-.022	.550	-.242	-.270	-.412	.285	.302	.360
.650	-.065	-.071	-.069	-.035	-.045	-.044	.650	-.259	-.270	-.414	.293	.294	.315
.750	-.055	-.072	-.082	-.054		-.055	.750	-.264	-.275	-.419	.262		.284
.825			-.086			-.061	.825			-.417			.271
.850	-.084	-.080		-.068	-.062		.850	-.274	-.286		.241	.247	
.900	-.097	-.082		-.079	-.067	-.056	.900	-.283	-.292		.235	.242	.233
.950	-.109	-.079					.950	-.271	-.293				
$\alpha = 4^\circ$							$\alpha = 16^\circ$						
0.050	-0.136	-0.139			0.216		0.050	-0.515	-0.543			0.722	
.075	-.117				.211		.075	-.475				.647	
.100	-.121	-.181	-0.130		.211		.100	-.436	-.522	-0.517		.590	0.650
.150	-.115		-.124	0.129	.175	0.243	.150	-.356		-.498	0.562		.596
.250	-.117	-.137	-.148	.097		.190	.250	-.308	-.507	-.486	.498		.552
.350	-.117	-.135	-.166	.077	.105	.142	.350	-.294	-.445	-.473	.460	.489	.513
.450	-.117	-.123	-.183	.067	.083	.118	.450	-.278	-.384	-.472	.417	.454	.473
.550	-.117	-.126	-.206	.067	.070	.103	.550	-.278	-.361	-.483	.421	.426	.420
.650	-.137	-.135	-.200	.047	.046	.077	.650	-.286	-.360	-.482	.415	.416	.386
.750	-.152	-.150	-.185	.028		.063	.750	-.300	-.365	-.484	.378		.365
.825			-.179			.056	.825			-.478			
.850	-.166	-.162		.027	.027		.850	-.317	-.358		.330	.351	
.900	-.172	-.168		.015	.024	.029	.900	-.322	-.352		.326	.344	.332
.950	-.178	-.166					.950	-.327	-.342				
$\alpha = 8^\circ$							$\alpha = 20^\circ$						
0.050	-0.289	-0.317			0.388		0.050	-0.580	-0.595			0.852	
.075	-.248				.382		.075	-.527				.794	
.100	-.236	-.333	-0.301		.315		.100	-.446	-.591	-0.593		.745	0.775
.150	-.209		-.291	0.266		0.393	.150	-.397		-.583	0.706		.716
.250	-.206	-.310	-.284	.234		.329	.250	-.363	-.539	-.572	.669		.667
.350	-.185	-.212	-.283	.181	.209	.275	.350	-.328	-.490	-.558	.621	.631	.621
.450	-.175	-.205	-.283	.156	.190	.243	.450	-.286	-.489	-.559	.568	.592	.574
.550	-.191	-.199	-.316	.170	.175	.223	.550	-.213	-.502	-.565	.552	.559	.520
.650	-.210	-.205	-.322	.162	.171	.197	.650	-.226	-.507	-.561	.525	.524	.479
.750	-.215	-.219	-.326	.132		.177	.750	-.251	-.478	-.560	.473		.455
.825			-.322			.155	.825			-.550			
.850	-.227	-.225		.128	.134		.850	-.263	-.440		.431	.450	
.900	-.229	-.234		.119	.130	.126	.900	-.273	-.436		.433	.434	.426
.950	-.234	-.233					.950	-.286	-.426				

TABLE IV.- PRESSURE COEFFICIENTS FOR BODY IN PRESENCE OF WING

(a) Fixed transition; $p_t' = 1,950$ lb/sq ft

x/l	$\alpha = 0^\circ$	$\alpha = 2^\circ$	$\alpha = 4^\circ$	$\alpha = 6^\circ$	$\alpha = 8^\circ$	$\alpha = 12^\circ$	$\alpha = 16^\circ$	$\alpha = 20^\circ$	x/l
Row A									
0.055	0.086	0.072	0.041	0.042	0.028	0.003	0.009	-0.013	0.055
.166	.033	.020	.012	.004	.002	-.004	-.007	-.039	.166
.277	-.007	-.017	.002	-.013	-.013	-.027	-.015	-.044	.277
.367	.005	-.006	-.005	-.015	-.024	-.017	-.043	-.070	.367
.387	.020	.011	.007	-.004	.000	.013	.002	-.027	.387
.415	.006	.004	-.007	-.012	-.009	-.023	-.035	-.049	.415
.443	.008	-.006	-.016	-.006	-.003	-.008	-.039	-.080	.443
.498	-.009	-.035	-.059	-.092	-.109	-.150	-.187	-.184	.498
.553	-.017	-.065	-.098	-.133	-.167	-.220	-.260	-.285	.553
.581	-.036	-.077	-.111	-.148	-.179	-.242	-.265	-.285	.581
.636	-.041	-.083	-.119	-.154	-.189	-.233	-.282	-.301	.636
.664	-.062	-.101	-.138	-.178	-.202	-.252	-.298	-.318	.664
.692	-.069	-.107	-.143	-.174	-.201	-.262	-.300	-.319	.692
.719	-.091	-.131	-.162	-.196	-.231	-.292	-.326	-.358	.719
.775	-.060	-.058	-.060	-.054	-.054	-.062	-.037	.013	.775
.830	-.057	-.035	-.023	-.014	-.005	.011	.019	.026	.830
.871	-.020	-.013	-.003	.001	.003	.031	.019	.015	.871
Row B									
0.166	0.019	0.015	0.014	-0.003	-0.023	-0.057	-0.085	-0.119	0.166
.277	-.001	-.016	-.018	-.017	-.034	-.061	-.086	-.147	.277
.367	-.022	-.032	-.046	-.050	-.073	-.081	-.114	-.197	.367
.387	.027	.014	.008	-.007	-.023	-.050	-.083	-.160	.387
.443	.007	-.020	-.048	-.069	-.091	-.148	-.191	-.265	.443
.498	-.008	-.047	-.074	-.116	-.152	-.222	-.287	-.392	.498
.553	-.082	-.073	-.111	-.147	-.184	-.261	-.329	-.421	.553
.609	-.038	-.075	-.111	-.154	-.195	-.273	-.342	-.432	.609
.664	-.073	-.111	-.145	-.186	-.227	-.319	-.392	-.459	.664
.719	-.062	-.081	-.095	-.107	-.112	-.134	-.170	-.217	.719
.830	-.039	-.027	-.028	-.026	-.023	-.017	-.020	-.034	.830
.871	-.050	-.036	-.027	-.023	-.021	-.014	-.028	-.139	.871
Row C									
0.055	0.084	0.083	0.075	0.070	0.048	-0.008	-0.076	-0.161	0.055
.166	.019	.009	.024	.007	-.020	-.082	-.163	-.275	.166
.277	.009	-.005	-.010	-.030	-.040	-.112	-.213	-.336	.277
.367	-.008	.002	-.007	-.030	-.056	-.141	-.251	-.349	.367
.692	-.032	-.030	-.032	-.040	-.053	-.099	-.099	-.166	.692
.719	-.035	-.036	-.036	-.043	-.055	-.052	-.070	-.126	.719
.775	-.052	-.056	-.060	-.063	-.064	-.083	-.117	-.189	.775
.830	-.070	-.069	-.072	-.086	-.101	-.142	-.191	-.243	.830
.871	-.047	-.043	-.048	-.058	-.064	-.075	-.092	-.129	.871
.954	-.085	-.083	-.088	-.094	-.097	-.119	-.129	-.139	.954

TABLE IV.- PRESSURE COEFFICIENTS FOR BODY IN PRESENCE OF WING - Continued

(a) Fixed transition; $p_t' = 1,950$ lb/sq ft - Concluded

x/l	$\alpha = 0^\circ$	$\alpha = 2^\circ$	$\alpha = 4^\circ$	$\alpha = 6^\circ$	$\alpha = 8^\circ$	$\alpha = 12^\circ$	$\alpha = 16^\circ$	$\alpha = 20^\circ$	x/l
Row D									
0.166	0.010	0.027	0.039	0.060	0.069	0.081	0.088	0.119	0.166
.387	.010	.016	.030	.030	.029	.011	.008	.019	.387
.443	.006	.026	.047	.055	.074	.133	.256	.396	.443
.498	.001	.045	.079	.115	.158	.255	.364	.492	.498
.553	.001	.045	.086	.138	.190	.280	.373	.486	.553
.609	-.025	.021	.066	.115	.163	.279	.385	.468	.609
.664	-.039	.007	.045	.091	.138	.251	.350	.414	.664
.719	-.055	-.035	-.016	.002	.024	.072	.109	.136	.719
.775	-.047	-.040	-.041	-.046	-.050	-.058	-.051	-.079	.775
.830	-.052	-.058	-.068	-.077	-.084	-.115	-.141	-.169	.830
.871	-.029	-.044	-.060	-.078	-.090	-.121	-.153	-.199	.871
Row E									
0.055	0.092	0.121	0.176	0.166	0.217	0.290	0.377	0.477	0.055
.166	.012	.037	.065	.093	.120	.206	.248	.347	.166
.277	.025	.037	.042	.042	.065	.123	.192	.278	.277
.367	.006	.024	.038	.057	.077	.118	.164	.240	.367
.387	.002	.018	.039	.051	.075	.114	.168	.235	.387
.443	-.003	-.002	.011	.019	.036	.079	.139	.205	.443
.498	.005	.053	.081	.122	.167	.273	.407	.547	.498
.553	.011	.054	.098	.158	.216	.313	.428	.546	.553
.609	-.016	.038	.089	.135	.173	.282	.400	.495	.609
.664	-.034	.007	.048	.102	.153	.268	.365	.445	.664
.719	-.067	-.026	.014	.061	.105	.190	.234	.276	.719
.775	-.044	-.035	-.020	-.013	-.007	.002	.033	.069	.775
.830	-.064	-.076	-.088	-.100	-.101	-.095	-.072	-.052	.830
.871	-.038	-.059	-.078	-.092	-.096	-.107	-.102	-.073	.871
.954	-.055	-.060	-.069	-.083	-.099	-.119	-.135	-.154	.954

TABLE IV.- PRESSURE COEFFICIENTS FOR BODY IN PRESENCE OF WING - Continued

(b) Natural transition; $p_t' = 1,950$ lb/sq ft

x/l	$\alpha = 0^\circ$	$\alpha = 4^\circ$	$\alpha = 8^\circ$	$\alpha = 12^\circ$	$\alpha = 16^\circ$	$\alpha = 20^\circ$	x/l
Row A							
0.055	0.089	0.043	0.028	0.003	0.008	-0.013	0.055
.166	.024	.010	.000	-.001	-.009	-.038	.166
.277	-.014	.004	-.015	-.027	-.018	-.054	.277
.367	-.001	-.002	-.022	-.016	-.036	-.054	.367
.387	.014	.011	.000	.009	.008	.002	.387
.415	-.008	-.005	-.006	-.027	-.027	-.030	.415
.443	.015	-.012	-.003	-.005	-.036	-.046	.443
.498	-.007	-.057	-.109	-.147	-.182	-.159	.498
.553	-.014	-.097	-.166	-.216	-.256	-.280	.553
.581	-.037	-.111	-.179	-.240	-.260	-.288	.581
.636	-.041	-.121	-.185	-.231	-.277	-.306	.636
.664	-.061	-.137	-.203	-.249	-.297	-.317	.664
.692	-.070	-.144	-.200	-.258	-.301	-.321	.692
.719	-.093	-.163	-.229	-.287	-.324	-.356	.719
.775	-.058	-.060	-.054	-.057	-.035	.011	.775
.830	-.057	-.019	-.003	.015	.022	.024	.830
.871	-.021	-.003	.002	.033	.025	.015	.871
Row B							
0.166	0.016	0.010	-0.024	-0.058	-0.084	-0.111	0.166
.277	-.009	-.019	-.035	-.060	-.086	-.133	.277
.367	-.011	-.046	-.073	-.083	-.115	-.222	.367
.387	.011	.007	-.024	-.050	-.084	-.184	.387
.443	.013	-.046	-.092	-.148	-.192	-.265	.443
.498	-.008	-.075	-.151	-.220	-.284	-.408	.498
.553	-.026	-.115	-.177	-.262	-.325	-.428	.553
.609	-.041	-.113	-.193	-.274	-.339	-.471	.609
.664	-.074	-.146	-.227	-.319	-.339	-.487	.664
.719	-.064	-.093	-.114	-.132	-.160	-.200	.719
.830	-.037	-.027	-.022	-.015	-.021	-.038	.830
.871	-.045	-.029	-.025	-.014	-.035	-.120	.871
Row C							
0.055	0.085	0.078	0.046	-0.003	-0.076	-0.159	0.055
.166	.019	.019	-.021	-.080	-.164	-.273	.166
.277	.000	-.010	-.040	-.109	-.214	-.335	.277
.367	-.018	-.006	-.056	-.138	-.249	-.370	.367
.692	-.031	-.036	-.055	-.101	-.106	-.187	.692
.719	-.034	-.038	-.054	-.049	-.070	-.177	.719
.775	-.051	-.060	-.064	-.078	-.118	-.171	.775
.830	-.070	-.074	-.101	-.136	-.191	-.243	.830
.871	-.044	-.053	-.060	-.069	-.088	-.124	.871
.954	-.085	-.089	-.099	-.118	-.127	-.143	.954

TABLE IV.- PRESSURE COEFFICIENTS FOR BODY IN PRESENCE OF WING - Continued

(b) Natural transition; $p_t' = 1,950$ lb/sq ft - Concluded

x/l	$\alpha = 0^\circ$	$\alpha = 4^\circ$	$\alpha = 8^\circ$	$\alpha = 12^\circ$	$\alpha = 16^\circ$	$\alpha = 20^\circ$	x/l
Row D							
0.166	0.011	0.037	0.063	0.077	0.084	0.118	0.166
.387	.000	.032	.030	.018	.013	.026	.387
.443	.003	.045	.060	.104	.254	.401	.443
.498	.004	.075	.160	.254	.361	.508	.498
.553	.008	.088	.193	.280	.368	.500	.553
.609	-.022	.065	.163	.282	.390	.474	.609
.664	-.036	.046	.137	.254	.352	.419	.664
.719	-.055	-.017	.025	.076	.110	.131	.719
.775	-.044	-.040	-.050	-.055	-.053	-.093	.775
.830	-.050	-.066	-.085	-.110	-.141	-.161	.830
.871	-.034	-.067	-.097	-.123	-.156	-.194	.871
Row E							
0.055	0.095	0.161	0.217	0.292	0.377	0.473	0.055
.166	.011	.057	.112	.188	.239	.338	.166
.277	.017	.030	.056	.118	.180	.265	.277
.367	.003	.036	.077	.120	.165	.240	.367
.387	-.011	.039	.063	.102	.155	.231	.387
.443	.003	.010	.039	.080	.139	.204	.443
.498	.014	.083	.169	.276	.407	.549	.498
.553	.016	.101	.218	.313	.430	.548	.553
.609	-.010	.090	.174	.284	.400	.495	.609
.664	-.031	.050	.154	.269	.365	.445	.664
.719	-.069	.015	.104	.195	.236	.277	.719
.775	-.043	-.023	-.008	.001	.032	.067	.775
.830	-.063	-.088	-.105	-.094	-.072	-.058	.830
.871	-.039	-.077	-.098	-.105	-.102	-.079	.871
.954	-.053	-.068	-.100	-.118	-.134	-.156	.954

TABLE IV.- PRESSURE COEFFICIENTS FOR BODY IN PRESENCE OF WING - Continued

(c) Fixed transition; $p_t' = 1,000$ lb/sq ft

x/l	$\alpha = 0^\circ$	$\alpha = 4^\circ$	$\alpha = 8^\circ$	$\alpha = 12^\circ$	$\alpha = 15^\circ$	$\alpha = 20^\circ$	$\alpha = 24^\circ$	x/l
Row A								
0.055	0.093	-0.049	0.026	0.003	0.005	-0.017	-0.035	0.055
.166	.028	.016	.001	-.010	.003	-.022	-.074	.166
.277	-.008	-.011	-.014	-.021	-.036	-.081	-.127	.277
.367	-.001	-.007	-.013	-.026	-.054	-.088	-.117	.367
.387	.016	.014	.008	.003	-.013	-.058	-.073	.387
.415	-.011	-.012	-.010	-.028	-.052	-.059	-.081	.415
.443	-.017	-.003	-.009	-.015	-.033	-.088	-.105	.443
.498	-.016	-.064	-.117	-.155	-.183	-.197	-.202	.498
.553	-.014	-.095	-.169	-.224	-.261	-.273	-.309	.553
.581	-.024	-.108	-.180	-.246	-.263	-.294	-.320	.581
.636	-.032	-.119	-.193	-.232	-.283	-.298	-.309	.636
.664	-.063	-.139	-.203	-.255	-.290	-.311	-.316	.664
.692	-.060	-.142	-.201	-.266	-.290	-.311	-.314	.692
.719	-.084	-.158	-.222	-.288	-.313	-.342	-.346	.719
.775	-.057	-.055	-.057	-.055	-.033	.009	.047	.775
.830	-.053	-.020	-.002	.007	.001	-.027	-.007	.830
.871	-.022	.005	.010	.017	-.011	-.041	-.043	.871
Row B								
0.166	0.023	0.015	-0.022	-0.076	-0.131	-0.160	-0.218	0.166
.277	-.006	-.020	-.036	-.062	-.083	-.104	-.215	.277
.367	-.006	-.041	-.065	-.087	-.101	-.193	-.312	.367
.387	.015	.012	-.014	-.046	-.061	-.139	-.246	.387
.443	-.006	-.048	-.095	-.140	-.187	-.273	-.290	.443
.498	-.014	-.082	-.148	-.227	-.303	-.403	-.465	.498
.553	-.021	-.114	-.179	-.262	-.311	-.409	-.510	.553
.609	-.029	-.121	-.202	-.267	-.331	-.430	-.475	.609
.664	-.066	-.149	-.222	-.297	-.367	-.469	-.490	.664
.719	-.058	-.094	-.111	-.143	-.203	-.224	-.282	.719
.830	-.035	-.033	-.020	-.025	-.013	-.047	-.152	.830
.871	-.044	-.022	-.021	-.015	-.023	-.055	-.171	.871
Row C								
0.055	0.091	0.090	0.047	-0.005	-0.063	-0.151	-0.212	0.055
.166	.018	.018	-.027	-.075	-.161	-.254	-.315	.166
.277	.003	-.010	-.044	-.120	-.213	-.329	-.357	.277
.367	-.013	-.008	-.057	-.153	-.272	-.364	-.318	.367
.692	-.031	-.038	-.060	-.107	-.131	-.165	-.258	.692
.719	-.017	-.036	-.051	-.057	-.057	-.076	-.123	.719
.775	-.051	-.059	-.059	-.081	-.103	-.126	-.186	.775
.830	-.061	-.075	-.102	-.136	-.163	-.219	-.357	.830
.871	-.041	-.040	-.054	-.066	-.093	-.124	-.186	.871
.954	-.079	-.082	-.092	-.122	-.133	-.167	-.159	.954

TABLE IV.- PRESSURE COEFFICIENTS FOR BODY IN PRESENCE OF WING - Concluded

(c) Fixed transition; $p_t' = 1,000 \text{ lb/sq ft}$ - Concluded

x/l	$\alpha = 0^\circ$	$\alpha = 4^\circ$	$\alpha = 8^\circ$	$\alpha = 12^\circ$	$\alpha = 16^\circ$	$\alpha = 20^\circ$	$\alpha = 24^\circ$	x/l
Row D								
0.166	0.019	0.045	0.061	0.091	0.093	0.119	0.162	0.166
.387	.004	.031	.021	.011	.007	.023	.061	.387
.443	-.002	.038	.032	.051	.096	.211	.541	.443
.498	-.005	.085	.169	.280	.394	.557	.691	.498
.553	-.004	.089	.199	.310	.438	.536	.652	.553
.609	-.026	.063	.168	.282	.400	.489	.592	.609
.664	.001	.086	.175	.278	.369	.442	.517	.664
.719	-.052	-.020	.021	.065	.098	.122	.138	.719
.775	-.044	-.041	-.048	-.058	-.064	-.075	-.086	.775
.830	-.045	-.061	-.086	-.117	-.141	-.149	-.165	.830
.871	-.020	-.052	-.082	-.115	-.145	-.172	-.182	.871
Row E								
0.055	0.101	0.178	0.216	0.289	0.387	0.479	0.589	0.055
.166	.017	.060	.111	.195	.245	.334	.435	.166
.277	.015	.036	.067	.116	.190	.268	.367	.277
.367	.003	.051	.079	.123	.177	.242	.336	.367
.387	-.001	.039	.061	.106	.160	.226	.311	.387
.443	-.001	.004	.015	.062	.125	.190	.263	.443
.498	.001	.080	.088	.152	.404	.595	.697	.498
.553	.010	.099	.225	.337	.465	.568	.672	.553
.609	-.015	.082	.182	.287	.411	.508	.607	.609
.664	-.035	.057	.152	.267	.367	.449	.527	.664
.719	-.064	.016	.106	.189	.242	.281	.320	.719
.775	-.040	-.026	-.011	.001	.031	.067	.112	.775
.830	-.054	-.085	-.099	-.095	-.077	-.049	-.012	.830
.871	-.030	-.065	-.090	-.102	-.095	-.064	-.033	.871
.954	-.051	-.067	-.098	-.124	-.134	-.142	-.116	.954

TABLE V.- PRESSURE COEFFICIENTS FOR BODY ALONE

[Transition fixed; $p_t' = 1,950$ lb/sq ft]

x/l	$\alpha = 0^\circ$	$\alpha = 2^\circ$	$\alpha = 4^\circ$	$\alpha = 6^\circ$	$\alpha = 8^\circ$	$\alpha = 12^\circ$	$\alpha = 16^\circ$	$\alpha = 20^\circ$	$\alpha = 24^\circ$	x/l
Row A										
0.055	0.082	0.062	0.056	0.035	0.017	0.007	0.003	-0.014	-0.018	0.055
.166	.048	.036	.022	.012	.021	.005	-.018	-.042	-.095	.166
.277	.002	.012	-.012	-.017	-.020	-.025	-.024	-.045	-.077	.277
.367	.004	.009	-.008	-.017	-.009	-.025	-.049	-.087	-.121	.367
.402	-.014	-.028	-.038	-.032	-.025	-.030	-.052	-.043	-.128	.402
.437	-.027	-.038	-.030	-.024	-.029	-.031	-.057	-.086	-.139	.437
.472	-.030	-.027	-.027	-.032	-.031	-.027	-.054	-.071	-.152	.472
.506	-.030	-.034	-.038	-.036	-.036	-.045	-.066	-.088	-.140	.506
.541	-.033	-.039	-.040	-.039	-.036	-.048	-.070	-.095	-.113	.541
.575	-.043	-.046	-.043	-.038	-.040	-.046	-.076	-.117	-.164	.575
.610	-.044	-.042	-.042	-.044	-.038	-.053	-.102	-.136	-.148	.610
.645	-.048	-.043	-.039	-.035	-.031	-.053	-.079	-.121	-.148	.645
.676	-.043	-.045	-.041	-.036	-.038	-.059	-.077	-.112	-.144	.676
.707	-.048	-.042	-.039	-.036	-.036	-.057	-.080	-.107	-.131	.707
.748	-.047	-.041	-.037	-.034	-.038	-.058	-.085	-.137	-.166	.748
.790	-.043	-.039	-.039	-.038	-.029	-.069	-.089	-.109	-.157	.790
.831	-.049	-.043	-.041	-.040	-.041	-.063	-.073	-.126	-.189	.831
.873	-.050	-.039	-.038	-.044	-.054	-.071	-.089	-.140	-.178	.873
.954	-.063	-.049	-.048	-.061	-.079	-.094	-.090	-.140	-.140	.954
Row B										
0.166	0.032	0.025	0.010	-0.003	-0.022	-0.050	-0.086	-0.127	-0.240	0.166
.277	-.002	-.004	-.010	-.027	-.033	-.067	-.086	-.137	-.237	.277
.367	-.026	-.031	-.033	-.049	-.054	-.071	-.109	-.191	-.258	.367
.402	-.001	-.005	-.016	-.022	-.024	-.050	-.088	-.186	-.249	.402
.437	-.020	-.027	-.033	-.031	-.047	-.063	-.099	-.183	-.262	.437
.472	-.028	-.034	-.033	-.041	-.047	-.068	-.101	-.171	-.219	.472
.506	-.027	-.033	-.045	-.046	-.052	-.072	-.105	-.157	-.200	.506
.541	-.029	-.040	-.039	-.045	-.056	-.077	-.090	-.129	-.211	.541
.575	-.046	-.041	-.043	-.051	-.057	-.079	-.105	-.155	-.202	.575
.645	-.041	-.041	-.046	-.050	-.056	-.071	-.102	-.134	-.187	.645
.676	-.046	-.050	-.052	-.053	-.057	-.079	-.108	-.145	-.198	.676
.707	-.056	-.053	-.053	-.053	-.056	-.078	-.105	-.140	-.209	.707
.748	-.050	-.047	-.047	-.047	-.053	-.069	-.097	-.139	-.197	.748
.790	-.049	-.039	-.041	-.045	-.052	-.070	-.094	-.138	-.178	.790
.831	-.042	-.043	-.046	-.047	-.049	-.066	-.090	-.140	-.171	.831
.873	-.051	-.049	-.048	-.047	-.055	-.072	-.092	-.136	-.160	.873
Row C										
0.055	0.087	0.086	0.076	0.072	0.038	-0.007	0.070	-0.163	-0.231	0.055
.166	.019	.027	.017	-.001	-.029	-.079	-.172	-.280	-.339	.166
.277	.010	.010	-.005	-.014	-.043	-.112	-.198	-.339	-.386	.277
.367	-.002	-.010	-.025	-.037	-.065	-.129	-.238	-.348	-.325	.367
.437	-.023	-.026	-.037	-.054	-.072	-.141	-.195	-.236	-.236	.437
.472	-.015	-.028	-.044	-.055	-.078	-.135	-.201	-.224	-.215	.472
.506	-.029	-.035	-.044	-.066	-.091	-.141	-.207	-.236	-.219	.506
.541	-.043	-.047	-.056	-.067	-.084	-.150	-.212	-.226	-.241	.541
.575	-.029	-.032	-.041	-.058	-.079	-.129	-.192	-.237	-.245	.575
.610	-.055	-.058	-.067	-.081	-.089	-.143	-.193	-.243	-.249	.610
.645	-.018	-.028	-.039	-.056	-.078	-.126	-.179	-.212	-.215	.645
.676	-.041	-.051	-.058	-.071	-.095	-.144	-.193	-.220	-.214	.676
.707	-.045	-.052	-.066	-.082	-.103	-.139	-.182	-.192	-.198	.707
.748	-.032	-.040	-.052	-.065	-.084	-.120	-.153	-.155	-.158	.748
.790	-.045	-.048	-.055	-.063	-.077	-.113	-.136	-.155	-.155	.790
.831	-.033	-.041	-.051	-.064	-.076	-.094	-.111	-.150	-.137	.831
.873	-.010	-.013	-.014	-.019	-.029	-.044	-.069	-.093	-.083	.873
.954	-.077	-.078	-.075	-.069	-.071	-.076	-.090	-.101	-.121	.954

TABLE V.- PRESSURE COEFFICIENTS FOR BODY ALONE - Concluded

[Transition fixed; $p_t' = 1,950$ lb/sq ft]

x/l	$\alpha = 0^\circ$	$\alpha = 2^\circ$	$\alpha = 4^\circ$	$\alpha = 6^\circ$	$\alpha = 8^\circ$	$\alpha = 12^\circ$	$\alpha = 16^\circ$	$\alpha = 20^\circ$	$\alpha = 24^\circ$	x/l
Row D										
0.166	0.029	0.038	0.052	0.061	0.069	0.081	0.097	0.121	0.158	0.166
.402	-.009	-.011	-.010	-.012	-.009	-.017	-.026	-.026	-.001	.402
.437	-.016	-.025	-.031	-.027	-.033	-.038	-.039	-.034	-.007	.437
.472	-.021	-.017	-.024	-.033	-.039	-.054	-.060	-.048	-.014	.472
.506	-.026	-.027	-.022	-.032	-.038	-.059	-.067	-.063	-.033	.506
.541	-.035	-.043	-.046	-.043	-.047	-.072	-.093	-.088	-.054	.541
.575	-.049	-.048	-.051	-.058	-.065	-.065	-.085	-.096	-.071	.575
.610	-.047	-.054	-.064	-.063	-.073	-.105	-.103	-.108	-.101	.610
.645	-.050	-.053	-.064	-.071	-.080	-.108	-.135	-.137	-.115	.645
.676	-.030	-.039	-.047	-.056	-.071	-.099	-.127	-.140	-.123	.676
.707	-.043	-.048	-.060	-.067	-.076	-.105	-.137	-.142	-.122	.707
.748	-.051	-.056	-.064	-.072	-.086	-.117	-.151	-.169	-.155	.748
.790	-.051	-.056	-.066	-.070	-.078	-.102	-.132	-.156	-.149	.790
.831	-.046	-.051	-.063	-.069	-.083	-.121	-.158	-.193	-.174	.831
.873	-.038	-.039	-.047	-.054	-.071	-.112	-.159	-.194	-.183	.873
Row E										
0.055	0.088	0.104	0.038	0.200	0.200	0.285	0.383	0.478	0.585	0.055
.166	.026	.048	.038	.093	.122	.183	.265	.341	.447	.166
.277	.014	.023	.031	.067	.075	.118	.186	.267	.370	.277
.367	.004	.012	.024	.049	.067	.106	.169	.247	.339	.367
.437	-.012	-.010	-.010	.003	.013	.060	.116	.186	.273	.437
.472	-.022	-.010	-.014	-.003	.011	.047	.102	.176	.263	.472
.506	-.026	-.028	-.010	-.002	.005	.038	.089	.151	.233	.506
.541	-.031	-.029	-.029	-.014	-.010	.022	.066	.132	.230	.541
.575	-.038	-.037	-.033	-.028	-.018	.029	.058	.118	.195	.575
.610	-.048	-.049	-.042	-.030	-.016	.001	.054	.107	.174	.610
.645	-.044	-.052	-.051	-.045	-.033	-.002	.038	.092	.170	.645
.676	-.045	-.046	-.046	-.046	-.044	-.014	.027	.079	.141	.676
.748	-.056	-.062	-.060	-.061	-.058	-.039	-.010	.046	.107	.748
.790	-.042	-.042	-.043	-.047	-.044	-.025	.000	.039	.098	.790
.831	-.067	-.079	-.074	-.093	-.089	-.080	-.056	-.011	.049	.831
.873	-.035	-.039	-.036	-.052	-.050	-.046	-.025	.009	.066	.873
.954	.062	.035	.008	.006	-.004	-.009	-.013	-.018	-.013	.954

TABLE VI.- WING SECTION DATA

[Fixed transition; $p_t' = 1,950 \text{ lb/sq ft}$]

α , deg	Section normal-force coefficient, c_n			Section pitching-moment coefficient, $c_{m,c/4}$		
	0.20b/2	0.40b/2	0.70b/2	0.20b/2	0.40b/2	0.70b/2
0	0.0123	0.0123	0.0135	-0.0033	-0.0041	-0.0036
2	.1194	.1290	.1594	-.0253	-.0264	-.0331
4	.2090	.2400	.3045	-.0453	-.0439	-.0566
6	.3194	.3587	.4535	-.0653	-.0655	-.0883
8	.4103	.4671	.5894	-.0833	-.0837	-.1186
12	.6026	.6961	.8000	-.1203	-.1257	-.1645
16	.7852	.9116	1.0052	-.1583	-.1740	-.2127
20	.9542	1.0974	1.1755	-.1963	-.2229	-.2486

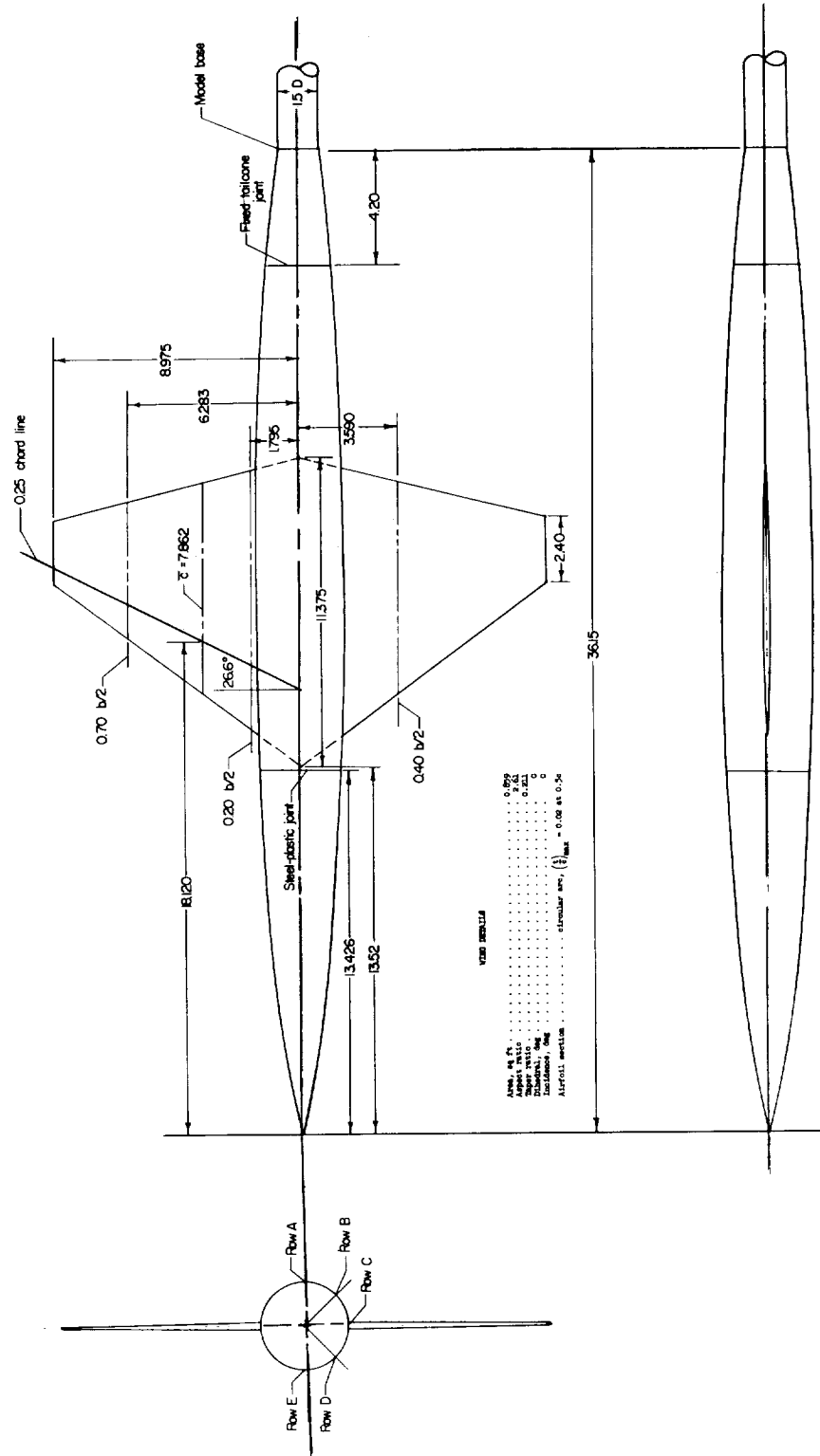


Figure 1.- Model details. All linear dimensions in inches unless otherwise noted.

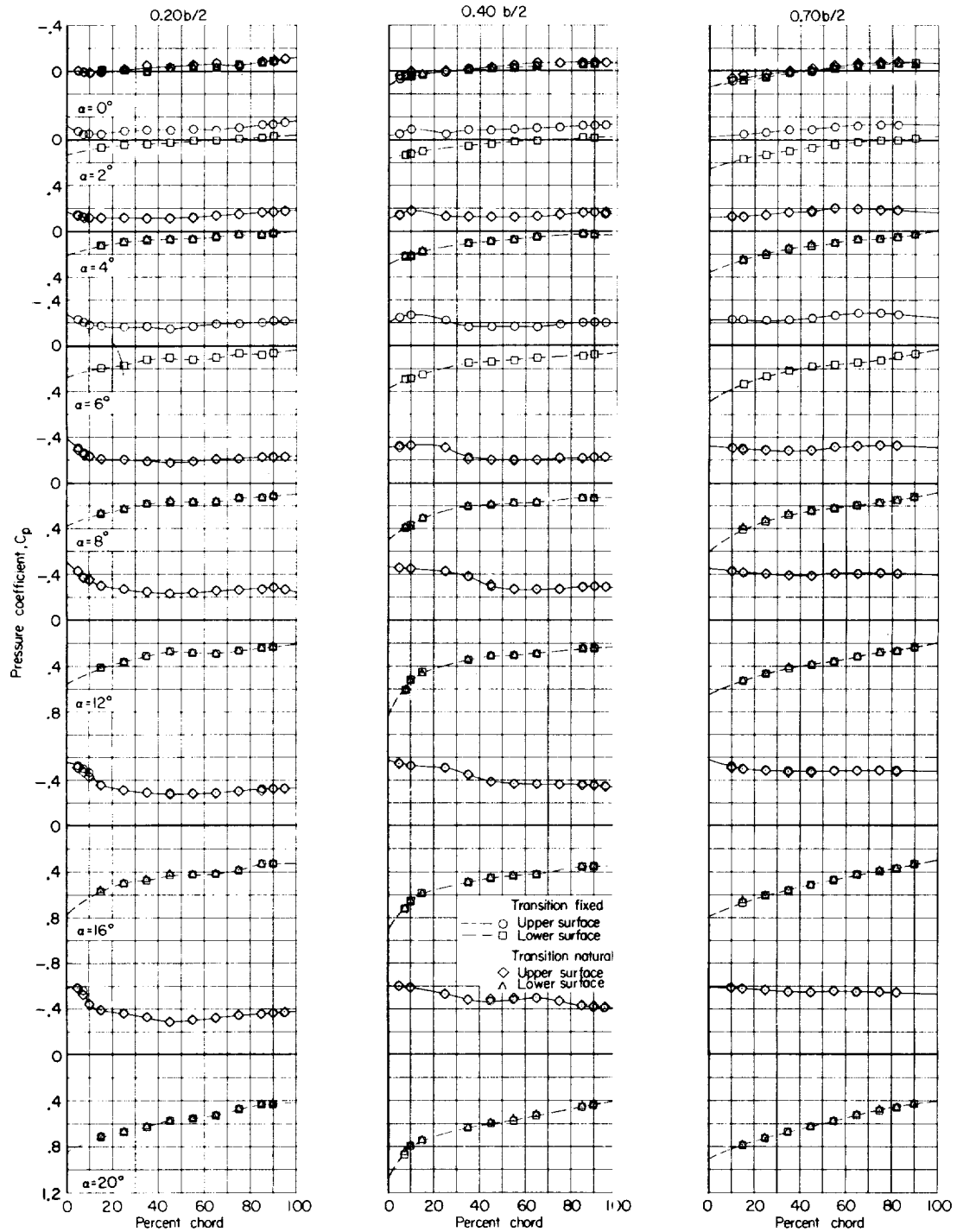
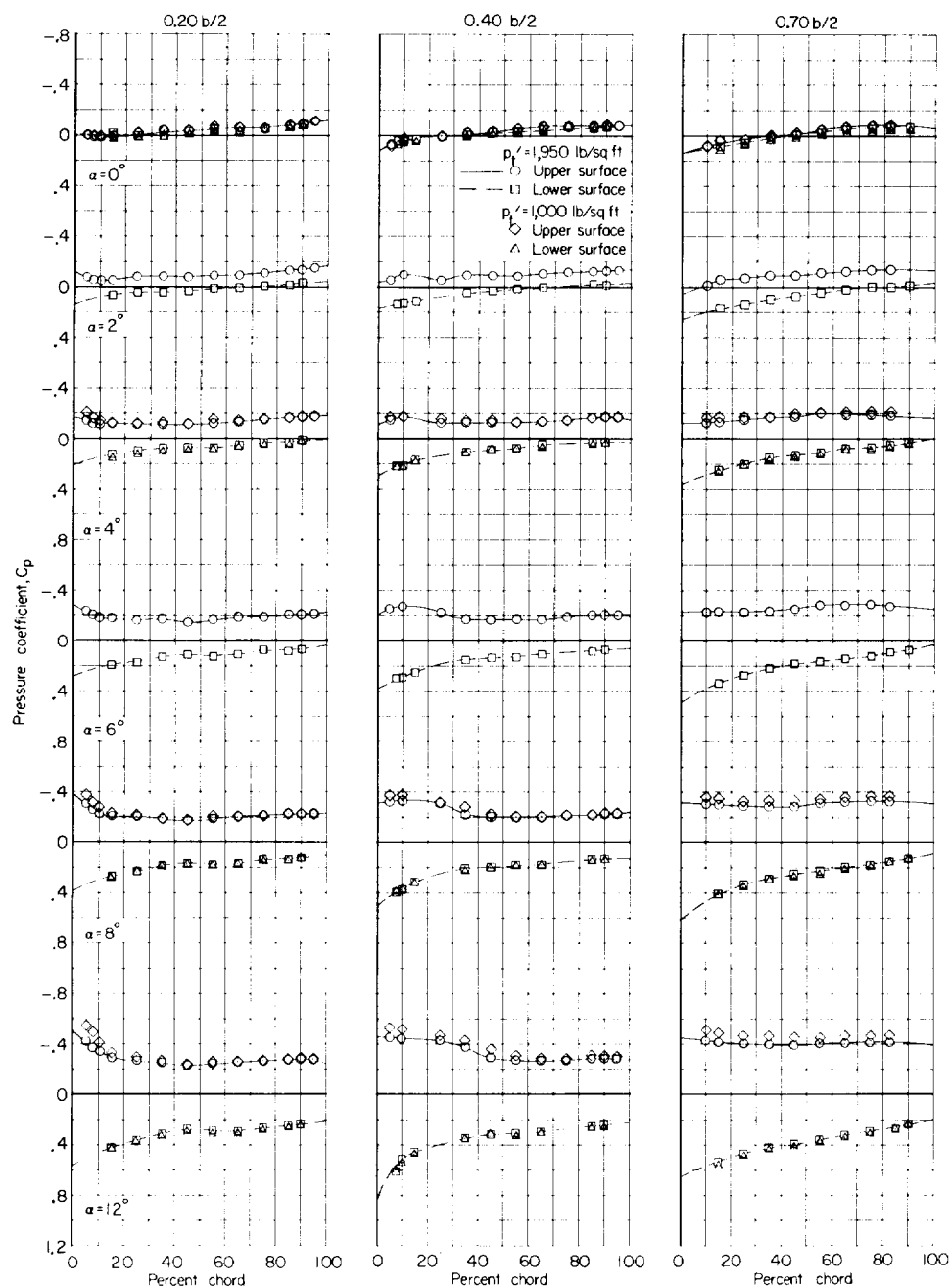
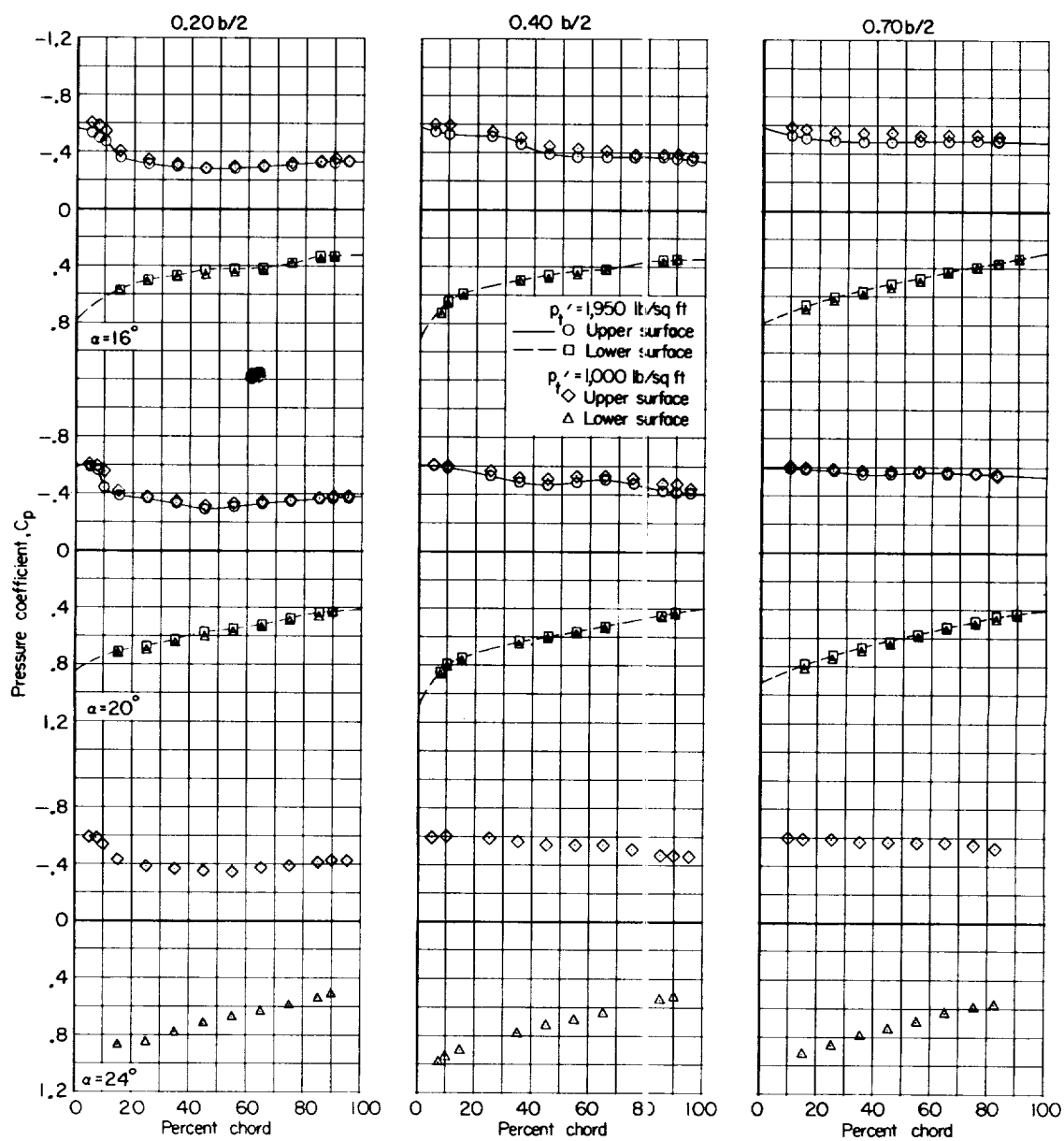


Figure 2.- Effect of transition on pressure coefficients for wing in presence of body. $C_{p, \text{sonic}} = 0.517$; $p_t' = 1,950$ lb/sq ft.



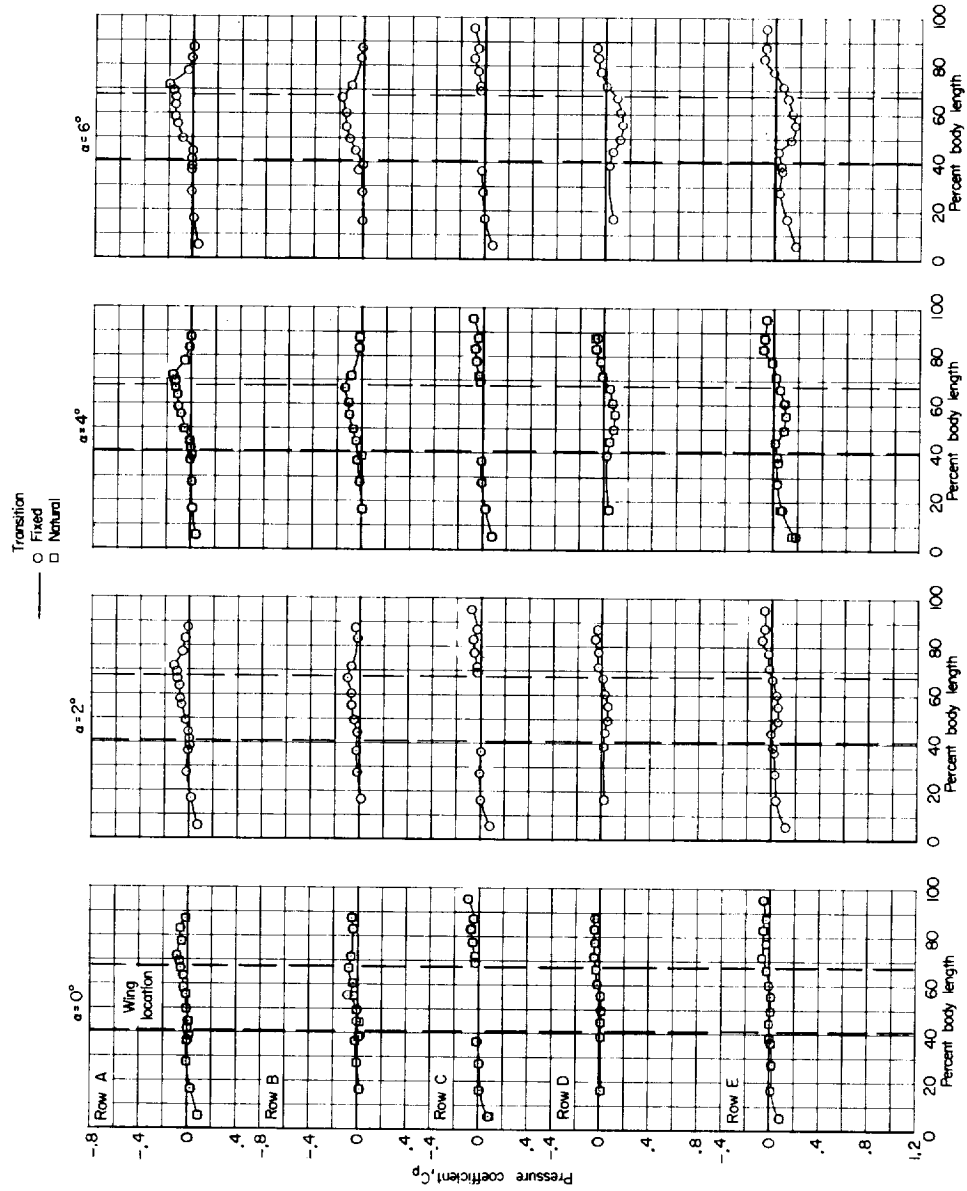
(a) $\alpha = 0^\circ, 2^\circ, 4^\circ, 6^\circ, 8^\circ$, and 12° .

Figure 3.- Effect of Reynolds number on pressure coefficients for wing in presence of body. $C_{p, \text{sonic}} = 0.517$; transition fixed.



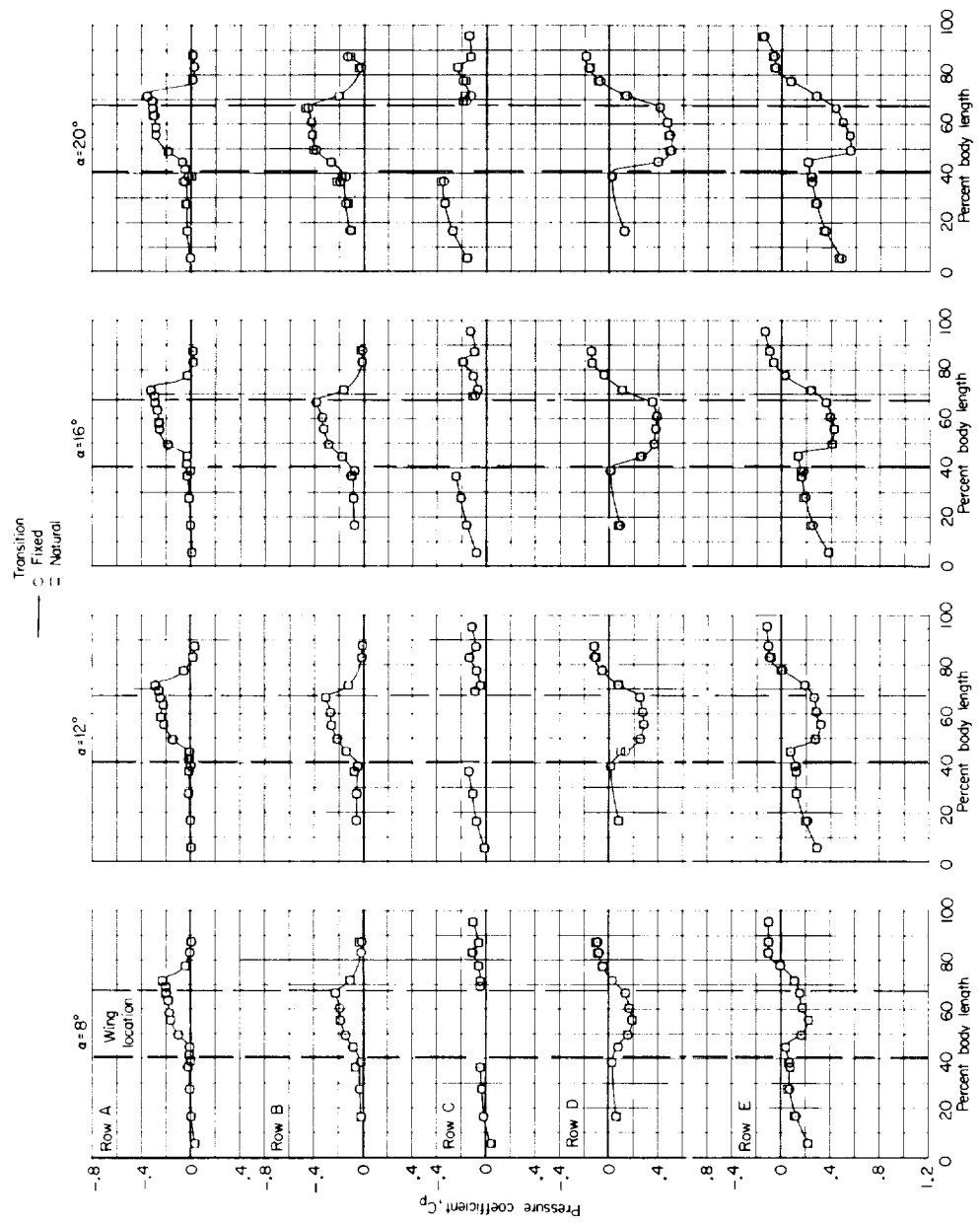
(b) $\alpha = 16^\circ$, 20° , and 24° .

Figure 3.- Concluded.



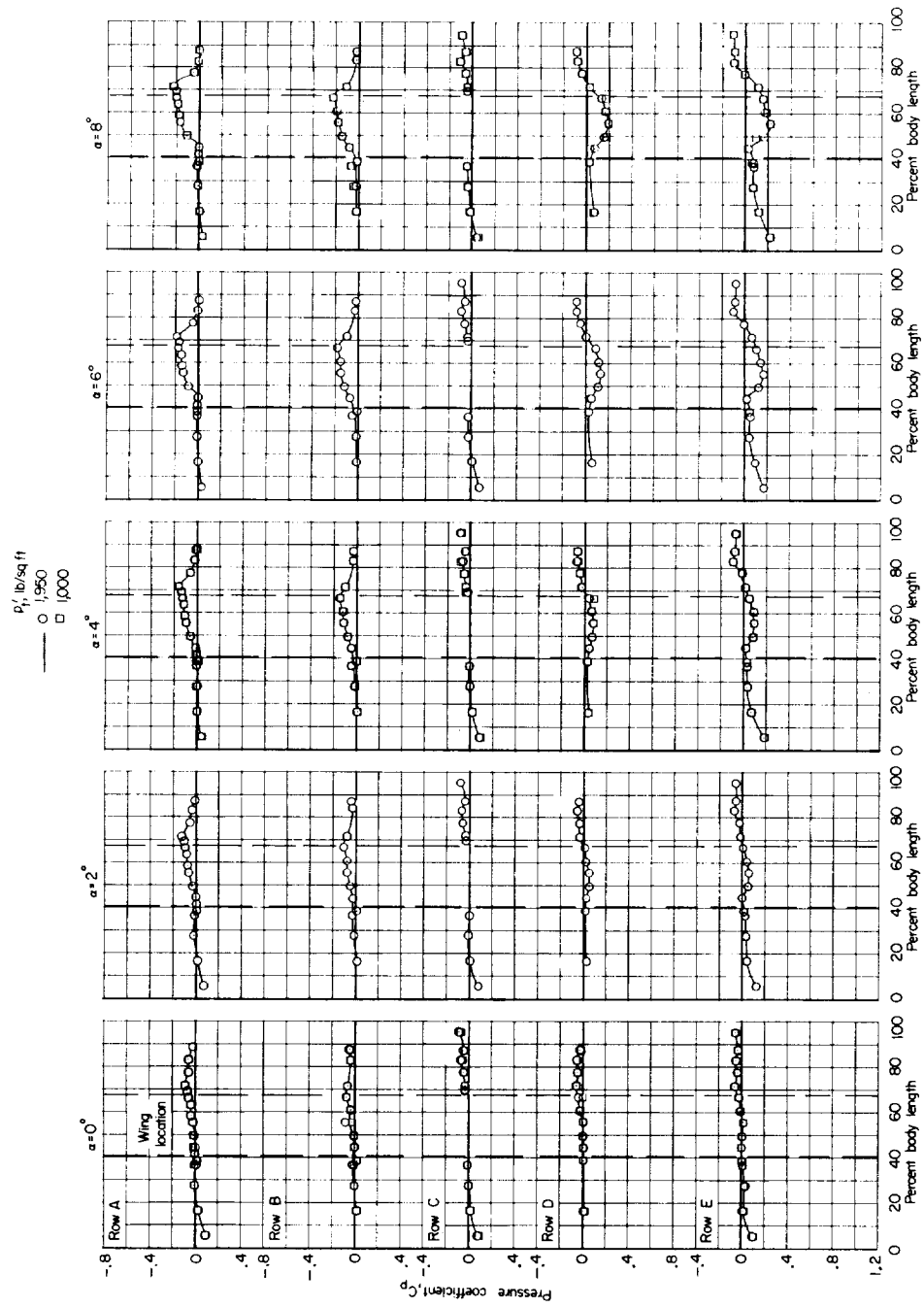
(a) $\alpha = 0^\circ, 2^\circ, 4^\circ, \text{ and } 6^\circ$.

Figure 4.- Effect of transition on pressure coefficients for body in presence of wing.
 $C_{p, \text{sonic}} = 0.517$; $P_t' = 1,950 \text{ lb/sq ft}$.



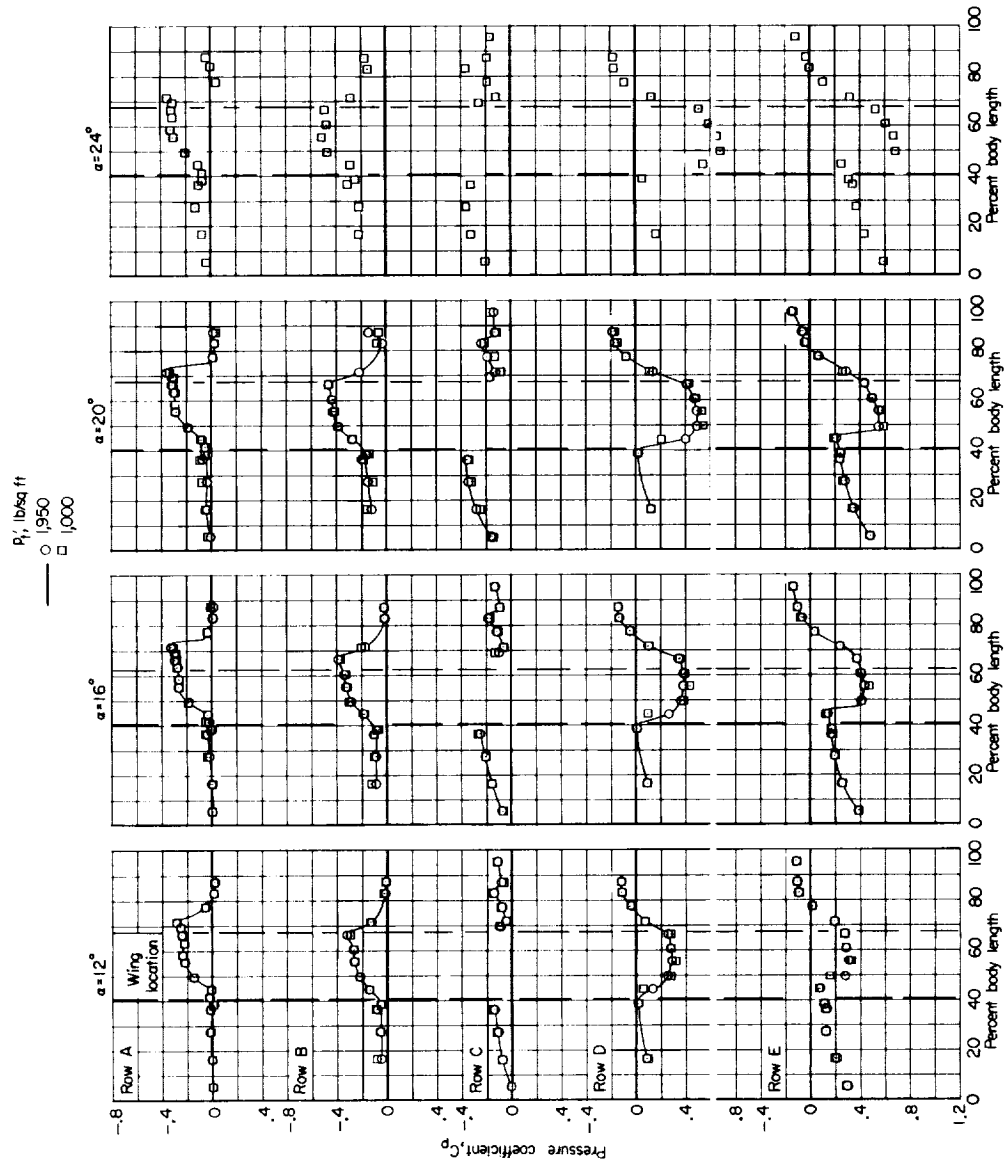
(b) $\alpha = 8^\circ, 12^\circ, 16^\circ$, and 20° .

Figure 4.- Concluded.



(a) $\alpha = 0^\circ, 2^\circ, 4^\circ, 6^\circ, \text{ and } 8^\circ$.

Figure 5.- Effect of Reynolds number on pressure coefficients for body in presence of wing.
 $C_{p, \text{sonic}} = 0.517$; transition fixed.



(b) $\alpha = 12^\circ$, 16° , 20° , and 24° .

Figure 5.- Concluded.

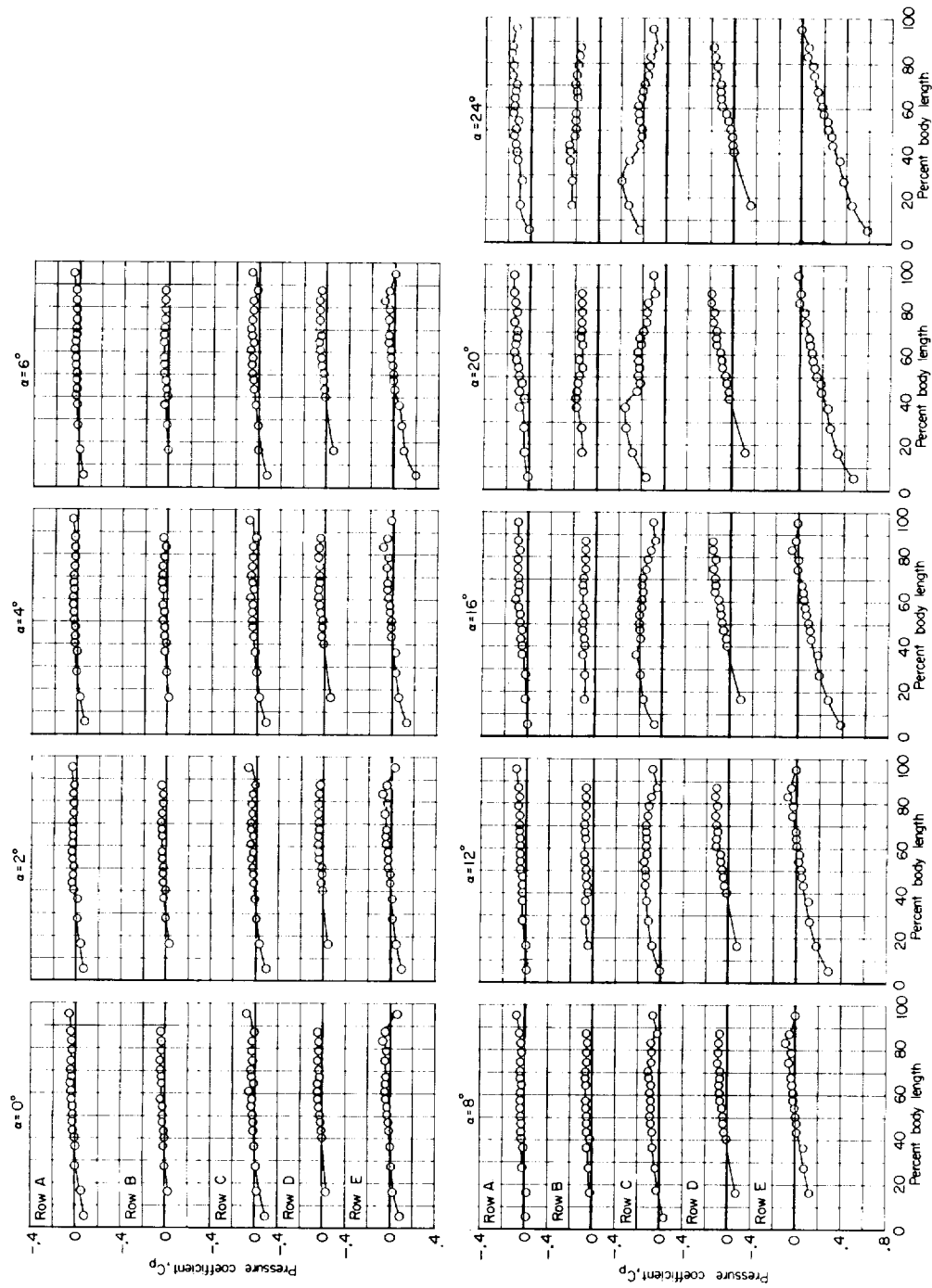


Figure 6.- Pressure coefficients for body alone. $C_{p, \text{sonic}} = 0.517$; $p_t' = 1.950 \text{ lb/sq ft.}$

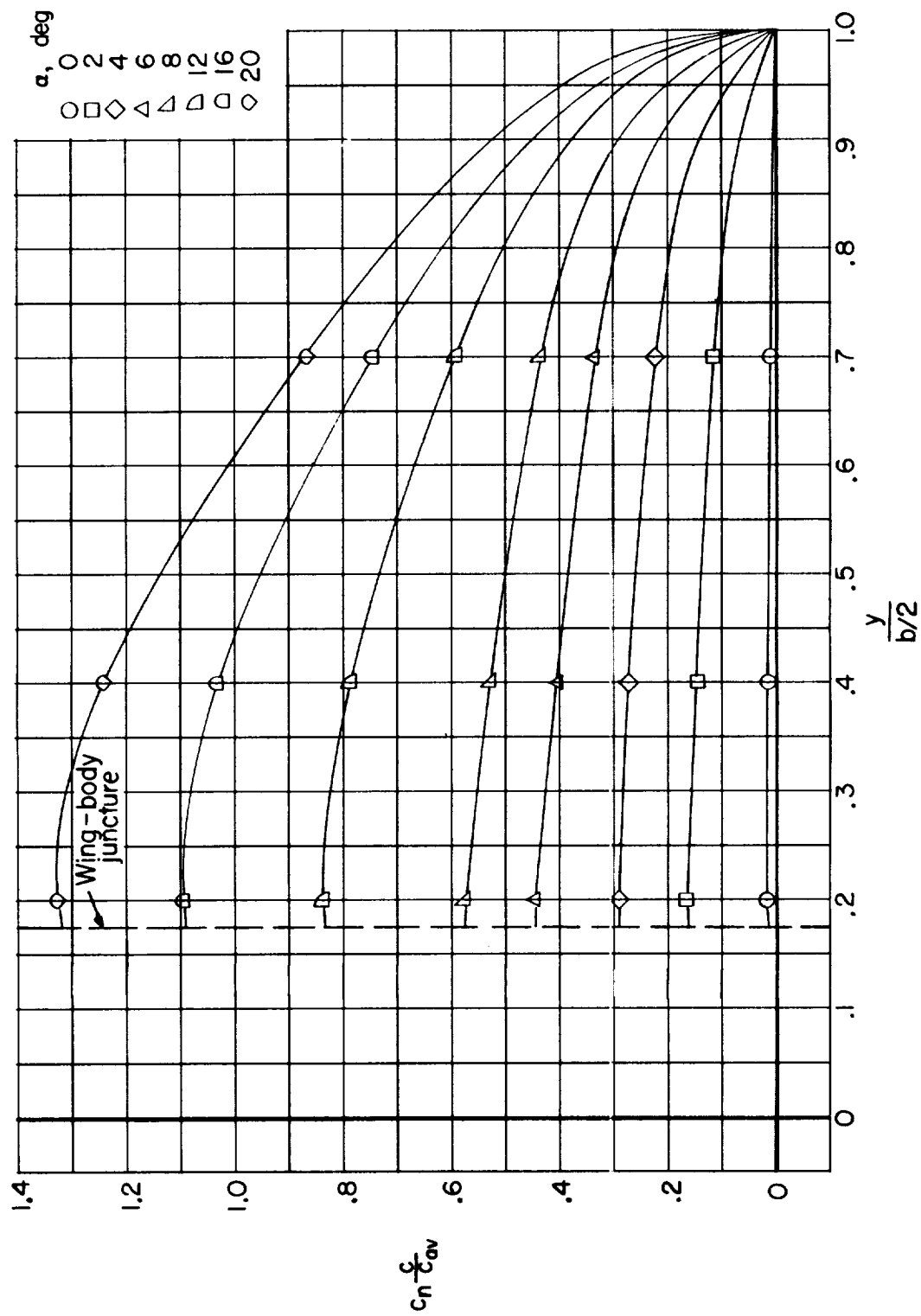


Figure 7.- Spanwise load distributions.

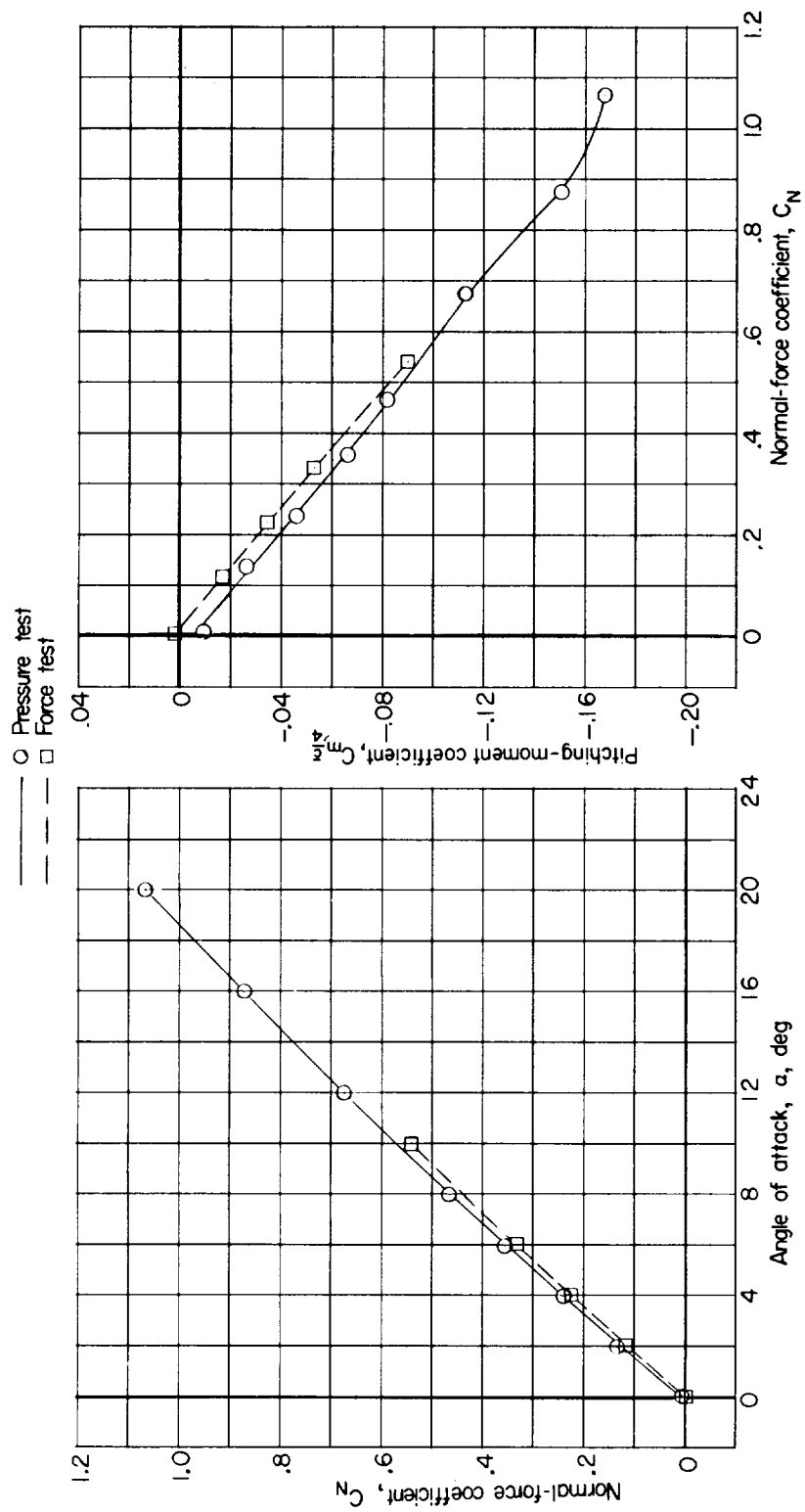


Figure 8.- Normal-force and pitching-moment characteristics of wing-body configuration.

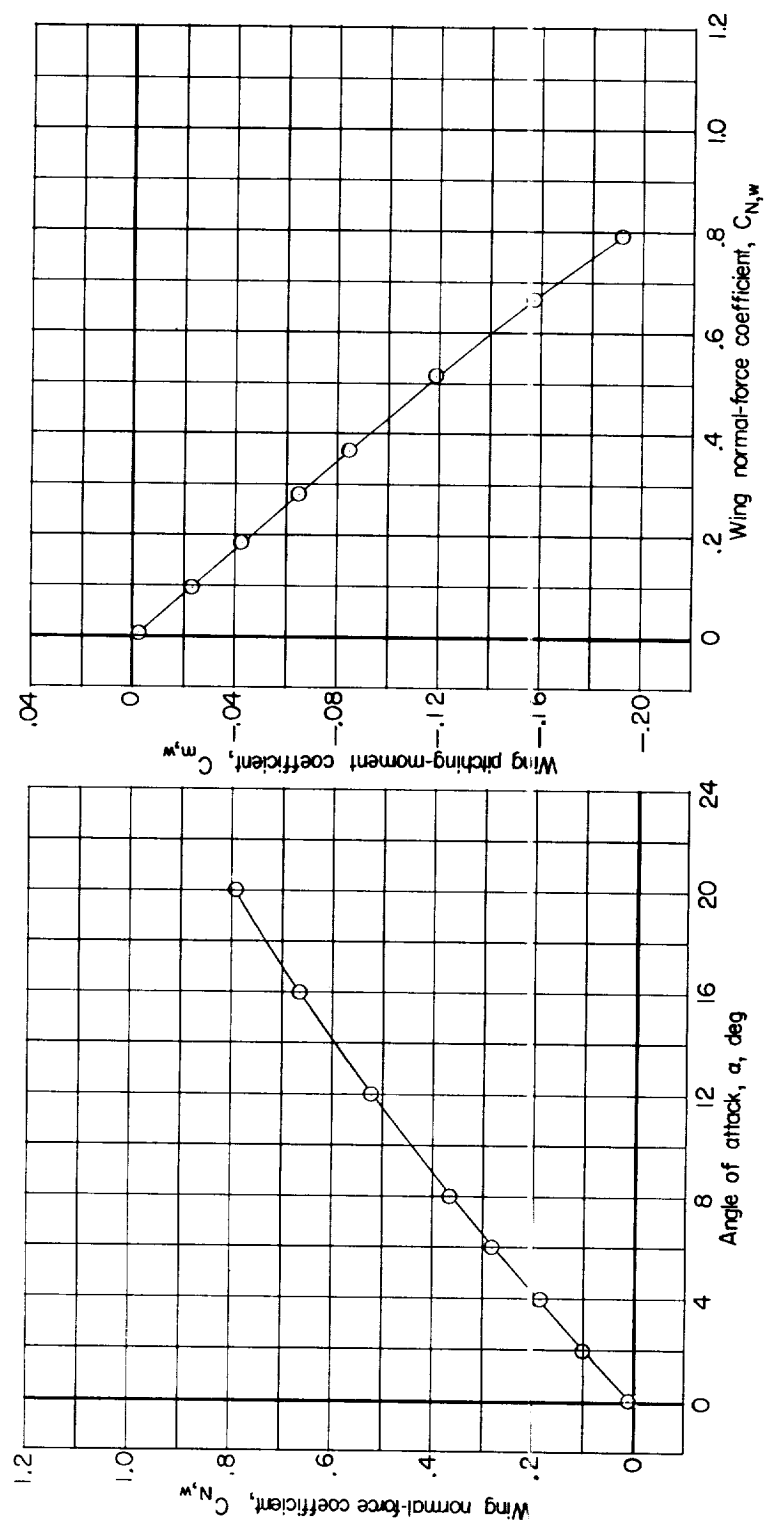


Figure 9.- Normal-force and pitching-moment characteristics of wing in presence of body.

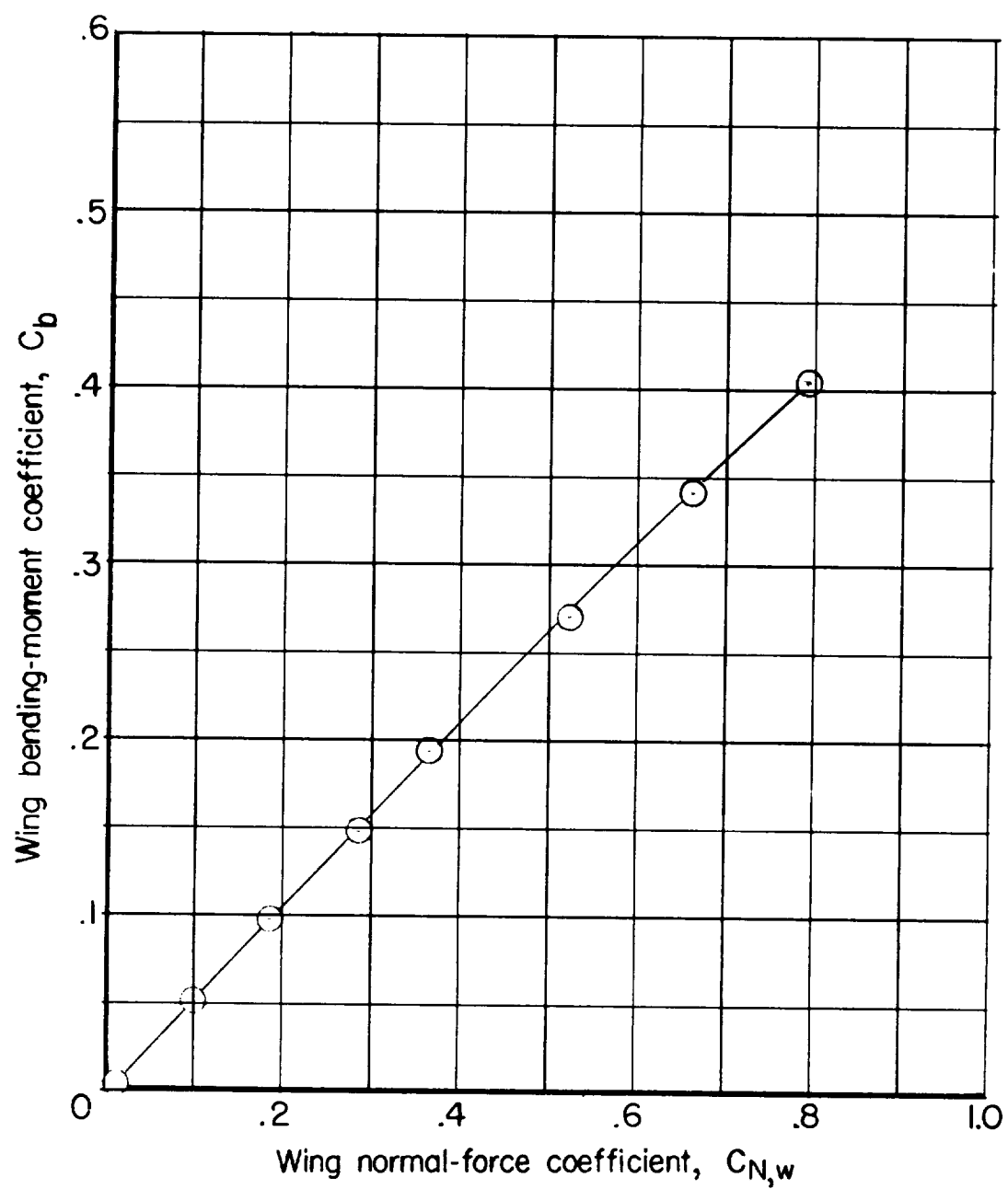


Figure 10.- Variation of wing bending-moment coefficient (referred to body center line) with normal-force coefficient.

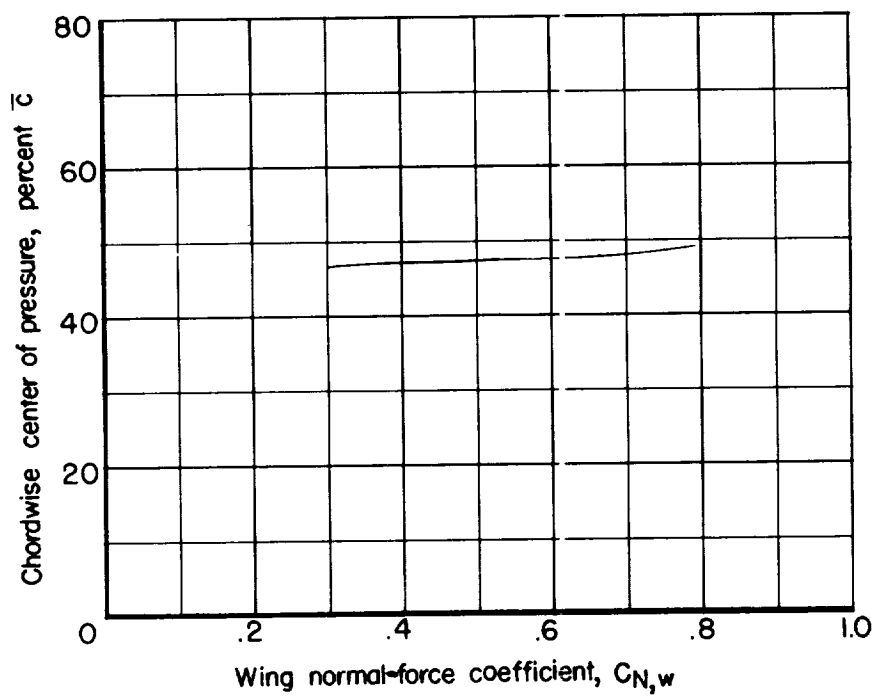
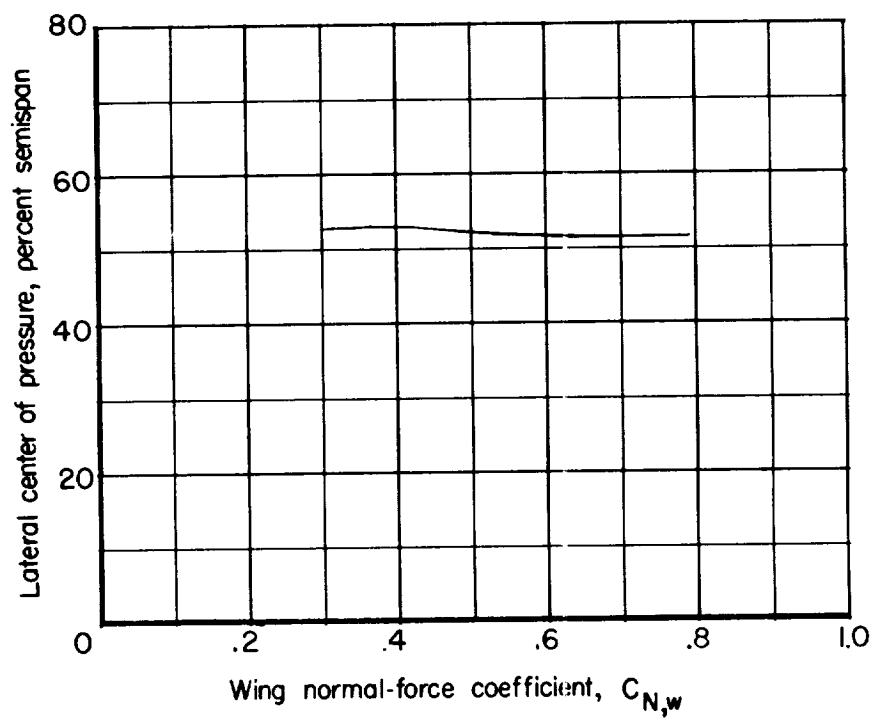


Figure 11.- Wing center-of-pressure locations.

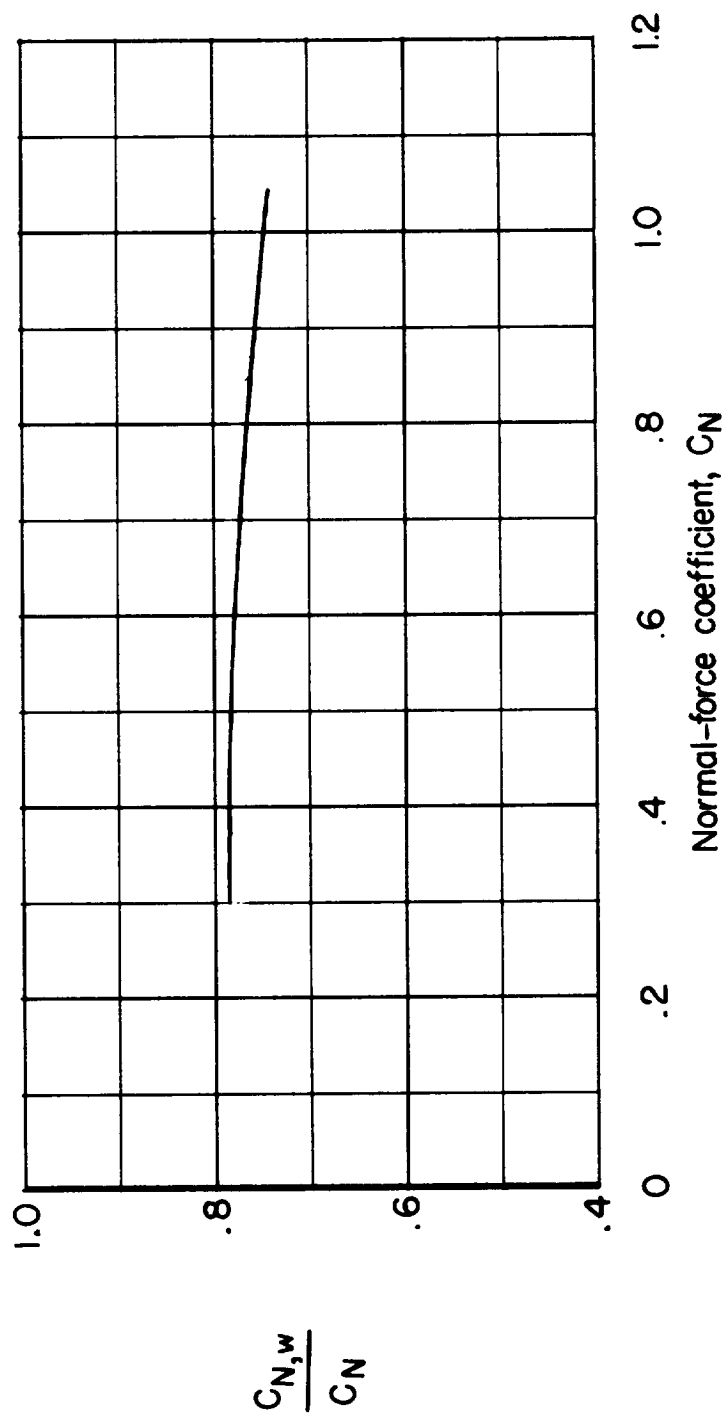


Figure 12.- Fraction of total load carried by wing.

